CONSULTANT REPORT

PIER
Public Interest Energy Research
CALIFORNIA ENERGY COMMISSION

Environmentally-Preferred
Advanced Generation

ANALYSES AND TECHNOLOGY TRANSFER FOR FUEL CELL SYSTEMS

Gray Davis, *Governor*

STATE OF CALIFORNIA
ENERGY COMMISSION
RESOURCES AGENCY

JUNE 2000

CALIFORNIA ENERGY COMMISSION

P600-01-00X

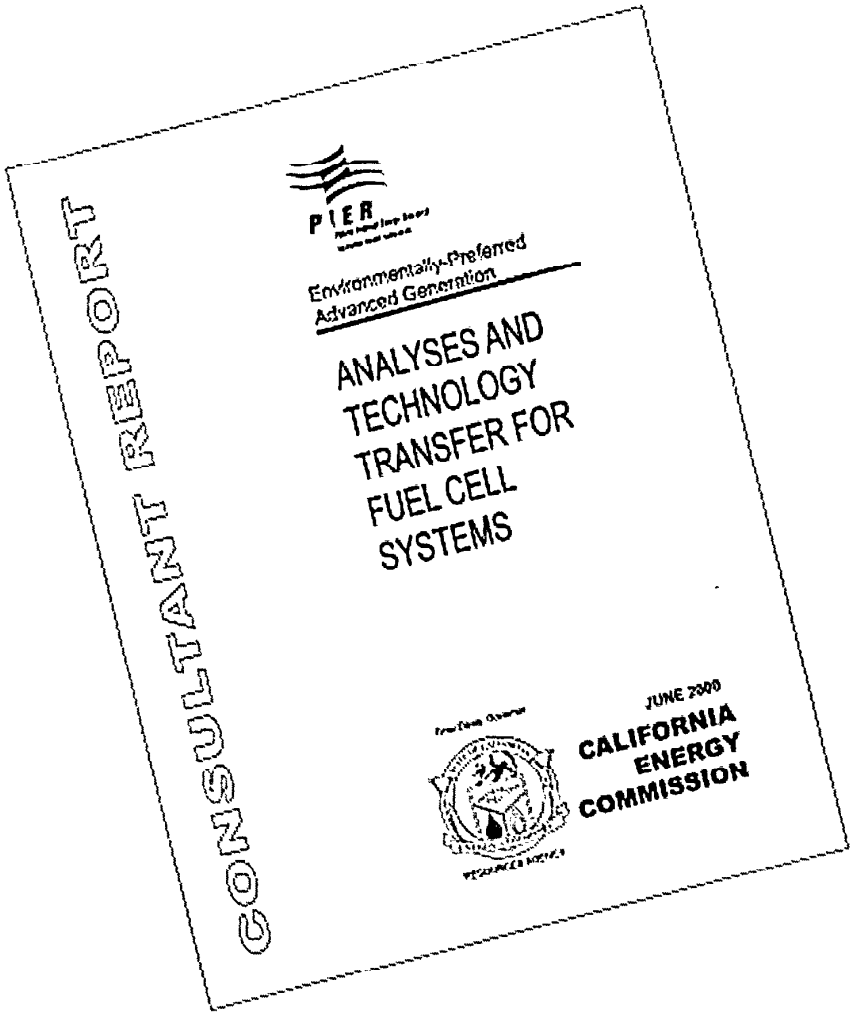

CALIFORNIA ENERGY COMMISSION

Prepared for:
CALIFORNIA ENERGY COMMISSION

Avtar Bining, *Contract Manager*
RESEARCH AND DEVELOPMENT OFFICE

Laurie ten Hope, *Team Lead*
STRATEGIC ENERGY RESEARCH

Prepared by:
Professor Scott Samuelsen

NATIONAL FUEL CELL RESEARCH CENTER
UNIVERSITY OF CALIFORNIA, IRVINE

Irvine, CA

Contract No. 500-98-052
Contract Amount: $305,733

Legal Notice

This report was prepared as a result of work sponsored by the California Energy Commission (Commission). It does not necessarily represent the views of the Commission, its employees, or the State of California. The Commission, the State of California, its employees, contractors, and subcontractors make no warranty, express or implied, and assume no legal liability for the information in this report; nor does any party represent that the use of this information will not infringe upon privately owned rights. This report has not been approved or disapproved by the Commission nor has the Commission passed upon the accuracy or adequacy of the information in this report.

Acknowledgements

The National Fuel Cell Research Center would like to acknowledge the following individuals for their significant contributions to the current effort:

Dr. Ashok D. Rao Ph.D. candidate during most of the current effort and primarily responsible for the development of the analyses tools modules

Mr. Matthew J. Traum Undergraduate student primarily responsible for the design and construction of the Educational Facility for Ambient Air Monitoring

Mr. William J. Skrivan Graduate student who accomplished much of the analyses tools results and comparison to data, and participated in the multi-functional room design and implementation

Mr. Craig S. Smugeresky Graduate student

Mr. Sandy Ryan South Coast Air Quality Management District contact person for ambient air monitoring station

Dr. Arthur J. Soinski California Energy Commission contract manager

Dr. Avtar Bining California Energy Commission contract manager

Dr. Jacob Brouwer University of California, Irvine project manager

Table of Contents

Appendices

List of Figures

Figure **Page**

List of Tables

Table **Page**

Preface

The Public Interest Energy Research (PIER) Program supports public interest energy research and development that will help improve the quality of life in California by bringing environmentally safe, affordable, and reliable energy services and products to the marketplace.

The PIER Program, managed by the California Energy Commission (Commission), annually awards up to $62 million to conduct the most promising public interest energy research by partnering with Research, Development, and Demonstration (RD&D) organizations, including individuals, businesses, utilities, and public or private research institutions.

PIER funding efforts are focused on the following six RD&D program areas:

- Buildings End-Use Energy Efficiency
- Energy-Related Environmental Research
- Environmentally-Preferred Advanced Generation
- Industrial/Agricultural/Water End-Use Energy Efficiency
- Renewable Energy
- Strategic Energy Research.

What follows is the final report for the Analyses and Technology Transfer for Fuel Cell Systems Contract, Contract Number # 500-98-052, conducted by the National Fuel Cell Research Center, University of California, Irvine, California. The report is entitled Analyses and Technology Transfer for Fuel Cell Systems. This project contributes to the Environmentally-Preferred Advanced Generation program.

For more information on the PIER Program, please visit the Commission's Web site at: **http://www.energy.ca.gov/research/index.html** or contact the Commission's Publications Unit at 916-654-5200.

Executive Summary

Although models for simulating the performance of natural gas steam reformation processes and gas turbine engines appear in the literature, analysis capabilities in the emerging field of solid oxide fuel cell and hybrid technologies were not available either in the literature or the marketplace. The development of these capabilities from the understanding of first principles was required.

Development of models for the reformer and gas turbine was also required since technologies intended for use in fuel cell hybrid systems differ significantly from traditional technologies that are amenable to current simulation software. The differences between gas turbines used in hybrid applications and those simulated with currently available software are fundamental and profoundly impact simulation capability and performance characteristics. To model these types of gas turbine and reformer systems, new simulation capabilities had to be developed and applied.

The overall goal of this project was to develop analysis strategies and technology transfer infrastructure for fuel cell systems and cycles, which can become a bridge between development, commercialization and successful deployment of the fuel cell technology. The project addresses the Public Interest Energy Research (PIER) program objective of reducing environmental and public health risks of California's electricity sector by helping develop environmentally preferred advanced generation technologies. It also contributes to the PIER program's objective of improving electrical system reliability by advancing fuel-cell technology for distributed electricity generation applications.

Objectives

The objectives of this project were to:

- Develop standard analysis tools for fuel cell systems and cycles
- Develop infrastructure for fuel cell technology transfer at the National Fuel Cell Research Center (NFCRC)

Outcomes

- The initial development of steady state analyses tools for fuel cell systems and cycles was completed with the development and demonstration of simulation modules for:
  - Tubular solid oxide fuel cell (SOFC)
  - Steam reformer
  - Gas turbine engine
- Technology transfer infrastructure for effective communication and information dissemination about fuel cells and fuel cell hybrid systems was accomplished in three separate areas:
  - Multi-Functional Room
  - Educational Facility for Ambient Air Monitoring (EFAAM)
  - NFCRC Web Site

Conclusions

Conclusions drawn from this project were:

- Preliminary results from the rigorous models developed in this effort are encouraging with regard to their ability to approximate conditions and results available in the literature without any adjustable parameters.
- The dependence of hybrid system components (SOFC, reformer, gas turbine) upon parametric variations is consistent with fundamental thermodynamics, efficiency expectations, and major loss mechanisms.
- The NFCRC has found the completed technology transfer features to be most valuable to effective communication and information dissemination, both within the fuel cell community and between the fuel cell community and other groups.

Benefits to California

The project addresses the PIER program objective of reducing environmental and public health risks of California's electricity sector by helping develop environmentally preferred advanced generation technologies. Fuel cells and fuel cell hybrid technologies offer a remarkable opportunity to reduce environmental impact, increase energy efficiency, and lower electricity costs in the future. These technologies, however, are significantly different from currently available energy technologies, and face many hurdles to their widespread adoption that can only be overcome by concerted efforts to transfer this technology from research, development and demonstration to applications in California.

Recommendations

We make the following recommendations:

- Funding the continued development of steady state analyses tools for fuel cells and fuel cell hybrid systems. Two additional years of funding support are required to finalize the analyses tools development, create a graphical user interface, and promulgate the use of these tools throughout the fuel cell community.
- Continued funding support of the out-years of the software development project to develop thermodynamic analysis tools for rigorous treatment, evaluation and design of fuel cells and hybrid systems.
- Current technology transfer efforts receive continued support from the California Energy Commission, and encourage other entities (e.g., industry, agencies, laboratories) concerned about the adoption of these technologies in the marketplace to expand their efforts in similar technology transfer endeavors.

Abstract

The National Fuel Cell Research Center (NFCRC) completed a one-year project, which accomplished the development of analyses strategies and tools for solid oxide fuel cells (SOFC) and fuel cell hybrid systems including a natural gas steam reformer and a gas turbine engine.

Simulation capabilities for a SOFC were required to advance the state-of-the-art. In addition, development of simulation capabilities for a gas turbine and reformer were also required since these systems, when used as components of a hybrid fuel cell gas turbine system, are significantly different from those of stand-alone steam reformation and gas turbine systems. Some differences to note for the gas turbine include: (1) single stage radial compressor and diffuser versus multistage axial compressor; (2) single stage radial turbine versus multistage axial turbine; (3) low pressure ratios; and (4) lower turbine inlet temperatures. Regarding the reformer, fundamental differences include: (1) intimate thermal integration of the reformer with the fuel cell stack, (2) lower temperature heat transfer to the reformer, (3) anode off-gas constituents differing significantly from pure steam, and (4) partial reformation without gas clean-up. To model these types of gas turbine and reformer systems, new simulation capabilities were developed and applied.

Simulation capabilities for an SOFC, a reformer, and a gas turbine engine were developed in the current program by using Quick Basic, Visual Basic, and C++ programming languages. The SOFC module simulates a tubular design based upon the fundamental mechanisms that govern fuel cell operation. The current model uses an integral approach that differs from models reported in the literature, which are based on finite element approaches. The gas turbine and reformer modules are based upon similar fundamental thermodynamic mechanisms as models found in the literature or in commercially available software packages, except customized for the simulation of hybrid systems.

Preliminary results from the rigorous models developed in this effort are encouraging with regard to their ability to simulate conditions and results available in the literature without any adjustable parameters.

NFCRC also accomplished technology transfer for fuel cell systems and cycles in the current effort. The NFCRC serves as an objective source for information on the state-of-the-art for fuel cells and other advanced power generation technologies. Technology transfer for fuel cells and fuel cell hybrid systems was accomplished in the current project in three separate areas: (1) multi-functional room development, (2) Educational Facility for Ambient Air Monitoring (EFAAM) installation and use, and (3) NFCRC Web-Site enhancement.

The new features of the multi-functional room have been used often to inform, educate, and communicate both within the fuel cell community and between the fuel cell community and other groups spanning regulatory bodies, government agencies, other industries, research institutions, and the general public.

Key Words: **fuel cell, solid oxide, thermodynamic analyses, hybrid, gas turbine, technology transfer**

1.0 Introduction

1.1 Background

Although models for simulating the performance of natural gas steam reformation processes and gas turbine engines appear in the literature, analysis capabilities in the emerging field of solid oxide fuel cell and hybrid technologies were not available either in the literature or the marketplace. Thus the development of these capabilities from the understanding of first principles was required.

Development of models for the reformer and gas turbine was also required since technologies intended for use in fuel cell hybrid systems differ significantly from traditional technologies that are amenable to current simulation software. The differences between gas turbines used in hybrid applications and those that can be simulated with currently available software are fundamental and profoundly impact the simulation capability and performance characteristics. These differences include: (1) single stage radial compressor and diffuser versus multistage axial compressor; (2) single stage radial turbine versus multistage axial turbine; (3) relatively low-pressure ratios; and (4) much lower turbine inlet temperatures.

Regarding the reformer, fundamental differences include: (1) intimate thermal integration of the reformer with the fuel cell stack, (2) lower temperature heat transfer to the reformer, (3) anode off-gas constituents differing significantly from pure steam, and (4) partial reformation without gas clean-up. To model these types of gas turbine and reformer systems, new simulation capabilities had to be developed and applied.

The overall goal of this project was to develop analysis strategies and technology transfer infrastructure for fuel cell systems and cycles, which can become a bridge between development, commercialization and successful deployment of the fuel cell technology. The project addresses the Public Interest Energy Research (PIER) program objective of reducing environmental and public health risks of California's electricity sector by helping develop environmentally preferred advanced generation technologies. It also contributes to the PIER program's objective of improving electrical system reliability by advancing fuel-cell technology for distributed electricity generation applications.

1.2 Budget Summary

Figure 1 shows the general cash flow estimates associated with this project. the California Energy Commission granted a no-cost time extension on December 15, 1999 to the contractor. Although the spending trend did not exactly track the projected expenditures, the project was completed within budget and in time, given the contract extension referenced above.

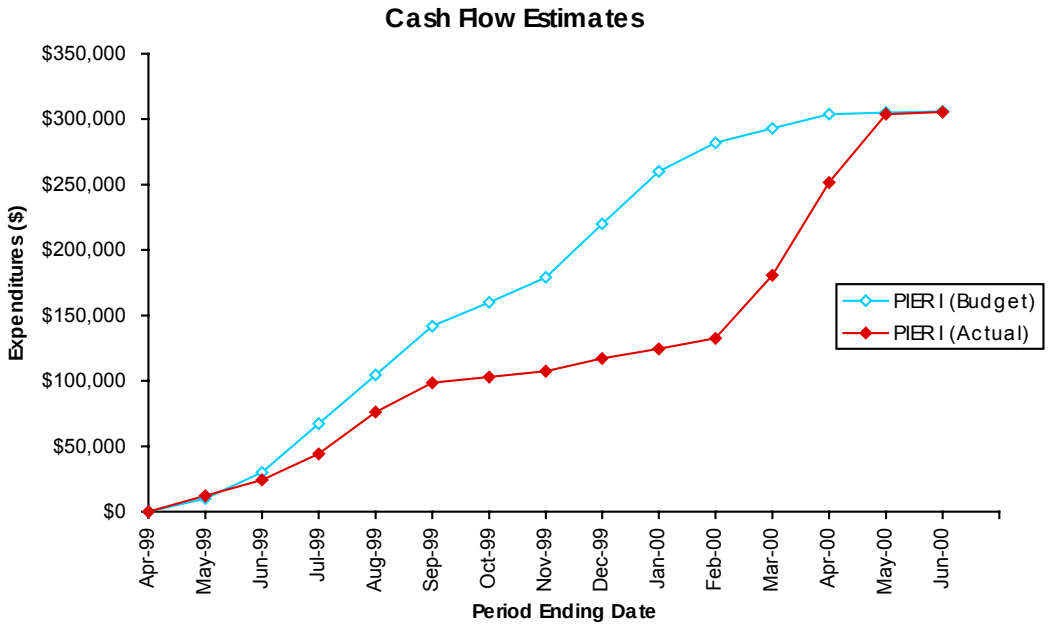

Figure 1. Cash Flow Budget Estimates and Actual Expenditures for the Current Project

1.3 Technical Tasks

The project's work scope involved two technical tasks: (1) Analyses of Fuel Cell Systems and Cycles, and (2) Technology Transfer. In the first technical task, Analyses of Fuel Cell Systems and Cycles, the National Fuel Cell Research Center (NFCRC) developed three modules that will serve as the basis of standard analysis tools that will be finalized in the second two years of an overall three-year effort. In addition to the modules, a draft standardized analysis format and energy tutorial were developed under this first technical task. The second task, Technology Transfer, involved the design installation and operation of advanced audio-visual, telecommunications, and meeting room accommodations to accomplish technology transfer for fuel cell systems and cycles. In this second technical task, the NFCRC developed, designed and installed specific infrastructure to assist in accomplishing this vision.

1.4 Project Objectives

The objectives of this project were to:

- Develop standard analysis tools for fuel cell systems and cycles
- Develop infrastructure for fuel cell technology transfer at NFCRC

Successful technology transfer would lead to the achievement of economic and competitive performance and successful market entry of advanced generation technologies such as fuel cells and fuel cell-microturbine hybrid systems. The direct project objective is therefore to develop technical analysis capabilities and technology transfer infrastructure at the NFCRC to enable the above to occur in subsequent years.

2.0 Task 1: Analysis of Fuel Cell Systems And Cycles

2.1 Introduction

Fuel cells are emerging as a stand-alone technology. Only one manufacturer currently offers a commercial fuel cell product (ONSI Corporation, PC-25™, 200 kW phosphoric acid fuel cell). Other fuel cell manufacturers are seeking to develop products for sale in the next two to five years. These products are still not defined and the development of "steady state" modeling tools could dramatically impact the designs that result from current developments in this emerging field. In addition, these tools are required for education purposes, both for undergraduate instruction and for graduate research and development.

The steady state tools could accomplish for stand-alone fuel cell systems, the analyses necessary to determine how one might best construct a fuel cell product to reduce complexity, while retaining reliability and reducing cost. The balance between these factors in the development of a product is difficult without the fundamental understanding of how processes and features of a system interact and work together to produce overall system features (e.g., efficiency, power output).

Hybrid fuel cell heat engine systems are at an earlier stage in their development with no demonstration of this technology to-date and no manufacturer offering a commercial fuel cell hybrid product. The proposed modeling tools could have a profound impact in this emerging area in that they will be used to determine critical path needs for the advancement of this technology, before they are tested in the field. In addition, the critical path research and development issues can be investigated and solved using the steady state analyses tools as applied to multiple variations in design and operating parameters. For hybrid systems, these critical path items include items as fundamental as a simple understanding of the cycle, identification of parameter ranges of interest (e.g., desired inlet and exit temperatures of FC and turbine streams), and the accurate determination of the effects of design and parameter changes on performance. In addition, these steady state tools provide fundamental insight into and guidance of experimental plans and results, through providing a scientific understanding of how and why observations occurred. Finally, these steady state tools can be used to educate a workforce for the development, manufacture, use, and maintenance of hybrid systems in the future.

The critical need of the fuel cell and hybrid fuel cell community is the acceleration and enabling of rapid advancement of technology along with enhancing the fundamental understanding and education of developers and users of this emerging technology. The current proposed tools directly address this critical need.

2.2 Background

Analysis capabilities in the emerging field of solid oxide and hybrid fuel cell technologies were not available either in the literature or the marketplace. Thus the development of these capabilities from the understanding of first principles was required. Although models for simulating the performance of natural gas steam reformation processes and gas turbine engines do appear in the literature and are available in some commercial simulation packages, these tools were not amenable to the simulation requirements of hybrid systems currently

undergoing research, development, and demonstration. This is due to several key factors that distinguish a fuel cell hybrid system from the traditional gas turbine cycle used for power generation, and the differences between the typical reformer plant used in refinery applications and that applied in a fuel cell hybrid application.

The differences between the gas turbine used in hybrid applications and that which can be simulated with currently available software are fundamental and profoundly impact the simulation capability and performance characteristics. These differences include:

- Single stage radial compressor and diffuser, vs., multistage axial compressor
- Single stage radial turbine vs. multistage axial turbine
- Relatively low pressure ratios (3-5 atmospheres vs. 20-50 atmospheres)
- Much lower turbine inlet temperatures

To model these types of gas turbine systems, a new simulation capability had to be developed and applied. This simulation capability was based upon the same fundamentals contained in available literature and commercial simulation packages with significant modifications and enhancements to facilitate the accurate modeling of hybrid gas turbine engine systems.

The differences between natural gas reformation processes accomplished in refinery applications, for example, are equally as far removed from those associated with the solid oxide fuel cell (SOFC) and SOFC hybrid systems. Software that is available or reported in the literature for natural gas reformation processes typically can model large hydrogen generation plants used for refinery, hydrogenation and other industrial processes. These systems, however, differ significantly from those contained in an SOFC system. First, the reformer in an SOFC system is typically integrated thermally into the fuel cell stack system to accomplish heat transfer from the stack to the reformer. This transfer of heat is accomplished at temperatures much lower than that associated with a typical reformer which uses direct firing (combustion) of natural gas to overcome the endothermicity of the reformation reactions. Second, the reformer in an SOFC system could also receive fuel cell stack anode off-gas and an input to supply the water (steam) required to accomplish the steam reformation chemical reactions. This anode off-gas typically contains many constituents other than steam that make the process much different than that associated with a typical steam reformation process. Third, the reformer used in an SOFC system only accomplishes a partial reformation of the natural gas to a hydrogen rich mixture. Fourth, the reformer used in an SOFC system does not contain the typical high temperature shift (HTS), low temperature shift (LTS), carbon monoxide (CO) polishing reactor, and pressure swing absorption (PSA) systems that are present to produce a pure hydrogen stream in the typical steam reformation system.

2.3 Approach

The platform in which the codes will be developed include workstation and personal computer platforms with the final product being amenable to use on both platforms.

Simulation capabilities for an SOFC, a reformer and a gas turbine engine were developed in the current program by using Quick Basic, Visual Basic, and C++ programming languages. These packages and their associated compilers were used to develop and produce simulation modules for each of the three components (SOFC, reformer, gas turbine) of a fuel cell hybrid system.

The SOFC module simulates a tubular design based upon the fundamental mechanisms that govern fuel cell operation. The model is superior to other models reported in the literature and contains a rigorous treatment of the major heat transfer mechanisms (conduction, convection, radiation), accurate accounting of pore diffusion & adsorption of oxygen (O_2) for cathode mass transfer, accurate accounting of all cell irreversibilities (activation, concentration, and ohmic polarization), and attention to fuel stream properties allowing consideration of hydrogen (H_2), CO, and hydrocarbons (CH_4), including shift reaction equilibrium considerations. Unlike the models in the literature, which are based on finite element approaches, the current model uses an integral approach.

The gas turbine and reformer modules are based upon similar fundamental thermodynamic mechanisms as models found in the literature or in commercially available software packages. The current gas turbine model is distinguished from these models by key features that are included in the current simulation: (1) radial and axial compressor designs and (2) blade cooling. The key features that distinguish the current reformer modeling capabilities from commercially available models include: (1) rigorous treatment of gas phase non-ideality, (2) multi-phase (gas-water) component considerations, and (3) capability to integrate the reformer into the SOFC system. Finally, the goal is to package these capabilities together in a user friendly in the out-years of this effort. This packaging will offer unique capabilities for the design and evaluation of hybrid systems not contained either in the literature, or in commercially available simulation software packages.

2.4 SOFC Technology

The electrolyte in a SOFC consists of a solid, nonporous metal oxide, typically yttrium oxide (Y_2O_3) stabilized zirconium oxide (ZrO_2) with the anode made from cobalt zirconium oxide ($CoZrO_2$) or nickel zirconium oxide ($NiZrO_2$) ceramic metal (cermet), while the cathode is made from strontium (Sr) doped lanthanum permanganate ($LaMnO_3$). At temperatures greater than 650°C oxygen ions ($O^=$) can be conducted through the electrolyte. Typically, this conduction is enhanced and certain losses are lowered at higher temperatures, which is why SOFCs are typically operated at temperatures above 800°C. The SOFC with its solid-state components may in principle be constructed in any configuration. Cells are being developed in tubular, flat plate and monolithic configurations. Figure 2 depicts the tubular SOFC stack schematically while Figure 3 shows the cross-section of an individual cell.

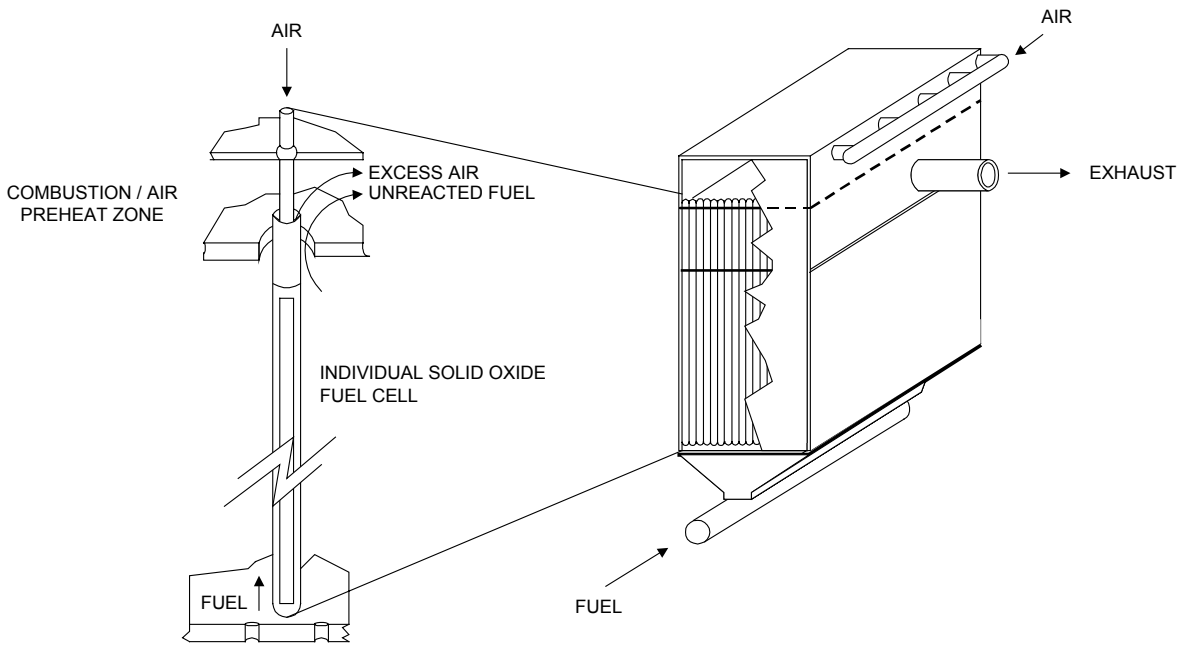

Figure 2. Schematic Representation of Tubular SOFC Stack (Bevc and Parker, 1995)

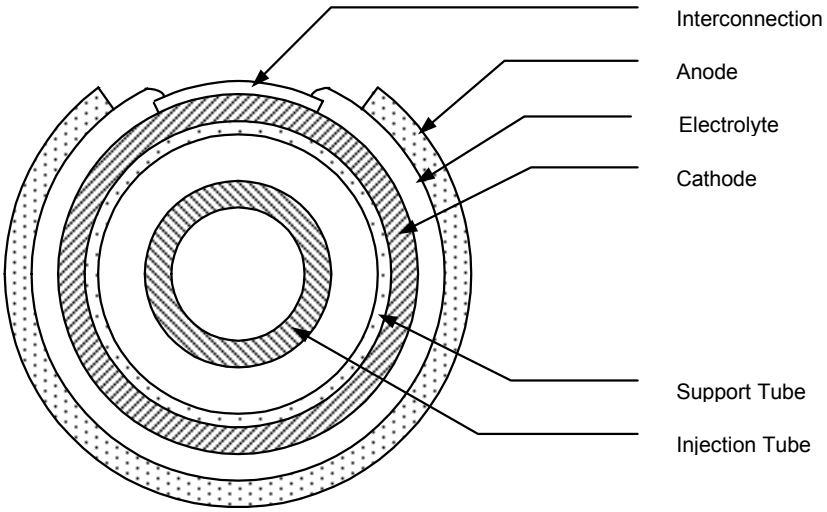

Figure 3. Cross-Section of an Individual Tubular SOFC (Hirschenhofer, et. al., January 1994).

An advantage of the SOFC is that internal reforming can be achieved with its high operating temperature that is typically around 1000°C. Also, the exhaust temperature of an SOFC is at high enough temperature and could be delivered at high pressures to allow conversion to power in a Brayton cycle (gas turbine cycle). This is the basic concept of the hybrid SOFC gas turbine cycle. One can use a Brayton cycle compressor to pressurize air (and fuel) going into the SOFC. The SOFC electrochemically converts much of the fuel energy to electricity, with the remainder producing heat that is available at the operating temperature of the fuel cell. This thermal exhaust is then typically used to pre-heat the incoming air and provide some heat to overcome the endothermic reactions that take place in the internal reformer of the fuel cell. The final thermal exhaust that leaves the SOFC section is available at lower temperatures (due to the heat transfer above) for powering the turbine of the Brayton cycle. The turbine in turn powers the compressor and an electric generator. There is sufficient thermal energy left in the SOFC exhaust stream to power both the compressor and an electric generator.

Considering the internal reformation process, one can assume that natural gas operation of the SOFC would lead to a hydrogen and carbon monoxide flow entering the fuel cell itself. The electrochemical reactions occurring within the cell for H_2 as the fuel are:

at the cathode: $1/2\ O_2 + 2e^- \rightarrow O^=$

at the anode: $H_2 + O^= \rightarrow H_2O + 2e^-$

with the overall cell reaction: $1/2O_2 + H_2 \rightarrow H_2O$

CO and hydrocarbons such as CH_4 can also be used as fuels in a SOFC. At the high temperatures within the cell, it is feasible for the water gas shift reaction: CO + water (H_2O) $\leftrightarrow$ H_2 + carbon dioxide (CO_2) and the steam reforming reaction: $CH_4 + H_2O \rightarrow 3H_2 + CO$ (in the case of natural gas) to take place to produce H_2 that is easily oxidized at the anode. The direct oxidation of CO in fuel cells is well established while the direct oxidation of CH_4 has not been

thoroughly investigated (Hirschenhofer, et al., January 1994). Any sulfur compounds present in the fuel have to be removed prior to use in the cell to a concentration of <0.1 parts per million by volume (ppmV).

2.4.1 SOFC Model Approach

Simulation capabilities for the SOFC were developed in the current program by using Quick Basic, Visual Basic, and C++ programming languages. These packages and their associated compilers were used to develop and produce a simulation module for the SOFC of a fuel cell hybrid system. The SOFC module simulates a tubular design based upon the fundamental mechanisms that govern fuel cell operation. The model is superior to other models reported in the literature and contains a rigorous treatment of the major heat transfer mechanisms (conduction, convection, radiation), accurate accounting of pore diffusion & adsorption of O_2 for cathode mass transfer, accurate accounting of all cell irreversibilities (activation, concentration, and ohmic polarization), and attention to fuel stream properties allowing consideration of H_2, CO, CH_4, including shift reaction equilibrium considerations. Unlike the models in the literature, which are based on finite element approaches, the current model uses an integral approach.

The overall strategy is to develop the necessary analytical and computational tools required for the development and analysis of SOFC based hybrid systems.

With the SOFC model developed in this research program, which accounts for the heat and mass transfer processes occurring within the cell as well as the electrochemistry, the calculated performance reflects the effect of the particular system design conditions such as fuel composition, operating pressure, fuel utilization and geometric parameters such as tube dimensions.

2.4.1.1 Thermodynamic Property Basis

The Peng-Robinson equation of state (Peng and Robinson, 1976), a modification of the van der Waals equation, is used to predict the deviations from non-ideality of the specific volume, enthalpy and entropy of gases. Peng and Robinson modified the attractive pressure term in the van der Waals equation was a significant improvement in the accuracy of property predictions. A dimensionless eccentric factor was introduced in the calculation of the attractive pressure term and the functional dependence on this factor was determined by using vapor pressure data. The critical property data presented by Reid et al. is used for calculating the two constants in the equation of state. The ideal gas properties are obtained from polynomials fitted to data published in JANAF Thermochemical Tables, 1985.

Empirical correlations developed by Schnackel (1958) are used for predicting the specific volume, enthalpy and entropy of pure steam. The properties of saturated water are predicted by empirical equations fitted to the ASME published data. A third degree polynomial fit is used relating the enthalpy to the saturated water temperature. A logarithmic relation is used to predict the entropy as a function of the saturated water temperature. The saturated vapor pressure of water is predicted utilizing the Antoine equation with the two constants empirically determined. For sub-cooled water, a correction to the saturated water properties is applied. This

correction factor is a function of the difference in the actual pressure and the saturated pressure of the water.

Vapor-liquid equilibrium is limited to pure water (liquid) and gas/water vapor mixture phases, that is, the solubility of any of the gas components in the liquid water phase is neglected. Raoults law under-predicts the moisture content of saturated gas mixtures at the lower temperatures. A relationship (equation (1)) that uses both the vapor pressure and the volume of saturated water vapor (which is obtained from the steam table data) is used:

$$y_{H2O} = Z_{dry\ gas} RT(P - P_s)/v_{H2O} \quad \textbf{(1)}$$

where y_{H2O} is moles of water vapor per mole of dry gas, $Z_{dry\ gas}$ is the compressibility factor of the dry gas determined by the Peng-Robinson equation of state, R is the universal gas constant, T the absolute temperature, P the system pressure, P_s the saturated vapor pressure of water and v_{H2O} is the specific molar volume of saturated water vapor at temperature T.

2.4.2 Tubular SOFC Model

An integral model for the heat and mass transfer and the electrochemical processes occurring in the various sections of the cell is developed although the model equations may be applied for zonal analysis of the SOFC when heat flux by conduction in the axial direction may be considered constant and inter-zonal radiation may be neglected. The integral model minimizes the computational time required to solve the SOFC module and thus the total time required by the computer to solve the entire hybrid plant. Note that a hybrid plant typically includes a number of other equipment modules and furthermore, a number of iterations have to typically occur not only within a module but also between the modules in order to arrive at a converged solution with all of the user-defined system design parameters satisfied.

The differential equations governing the various processes for a single cell are formulated and simplifying assumptions are made in order to solve these equations analytically. The resulting solutions to these equations are coded into the module. The net alternating current (AC) power output from the stack is estimated by applying an empirical factor to the product of the direct current (DC) power generated by a single cell and the total number of cells calculated.

The cell consists of an alumina central injector or air preheat tube in which the air is preheated before it enters the annular space between the injection tube and the cathode surface (Figure 4). Figure 3 depicts the cross-section of the cell. In older designs a substrate layer is included (innermost layer of the cell) adjacent to the cathode layer to provide structural support to the tubular cell. The solid electrolyte layer follows the cathode layer. The anode forms the outermost layer. Table 1 presents some of the cell dimensions. Some of the dimensions are shown as functions of the cell diameter (in equation form developed from data from the cited sources) so that the cell diameter may also be varied in order to assess its effect on the cell performance.

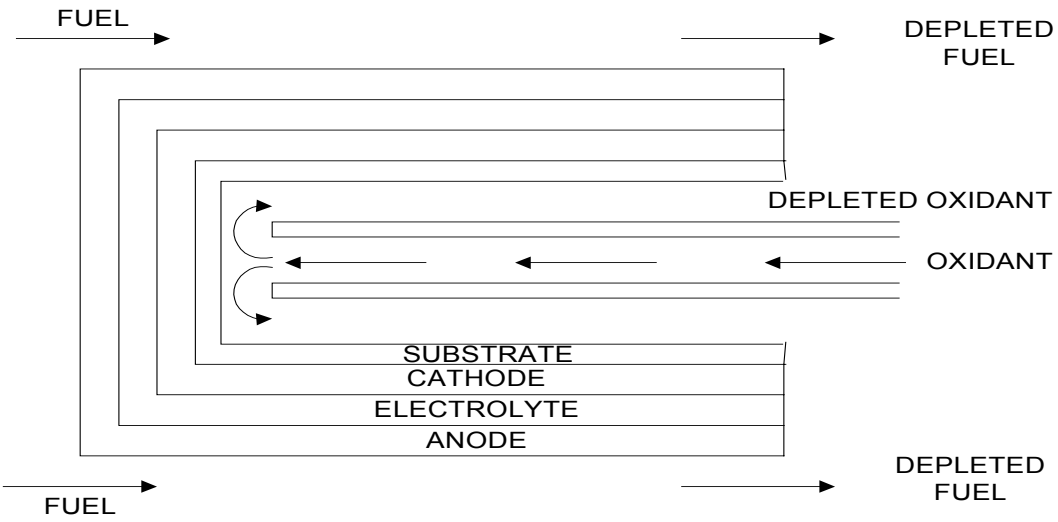

Figure 4. Schematic Cross Section of a Tubular SOFC

Table 1. Model Assumptions Regarding Individual SOFC Dimensions

Parameter	Dimension	Basis
Inside Diameter of Oxidant Preheat Tube	0.5 x Inside Cell Diameter	Hirano (1992) and correlating data from Bessette and George (1996)
Thickness of Oxidant Preheat Tube	0.17 x Inside Cell Diameter	Hirano (1992) and correlating data from Bessette and George (1996)
Inside Diameter of Cell	1.76 cm	Bessette and George (1996)
Thickness of Substrate Layer (if any)	0.001 cm	Hirschenhofer et al. (1994)
Thickness of Cathode Layer	0.05172 x Inside Cell Diameter + 0.12897 cm	Correlating data from Bessette and George (1996)
Thickness of Electrolyte Layer	0.004 cm	Hirschenhofer et al. (1994)
Thickness of Anode Layer	0.011 cm	By difference from data presented by Bessette and George (1996)
Pitch (distance between center of Tubes)	1.05 x Outside Cell Diameter	Estimated form drawing in Fuel Cell Handbook, Appleby and Foulkes, (1993)

The following sections summarize the approach taken, the equations derived and the assumptions made in the various sections of the cell simulation.

2.4.2.1 Heat Transfer

Heat Transfer from the Injector Tube Inside Surface to Oxidant. Both convective and radiant heat transfer in the radial direction are taken into account between the injector (air preheat) tube inside surface and the oxidant while assuming the oxidant to be a gray gas. Axial symmetry is assumed and heat flux by conduction in the axial direction is neglected in the gas due to its relatively low thermal conductivity while for the solid is assumed constant (that is, temperature is assumed to vary linearly in the axial direction). With these assumptions, the heat transfer equation for a differential element taken in the axial direction (Figure 5) reduces

$$dQ_1/dz = \pi D_i [h_i (T_S - T_G) + \sigma \varepsilon (T_S^4 - T_G^4)] \quad \textbf{(2)}$$

where T_S is the temperature of the inside solid surface, T_G is the temperature of the oxidant, Q_1 is the heat transferred to the oxidant (determined by an enthalpy balance, $dQ_1 = dH_{G1}$, where dH_{G1} is the increase in enthalpy of the oxidant), D_i is the inside diameter of the injector (air preheat) tube, σ is the Stefan-Boltzmann constant, $\varepsilon = 1/(1/\varepsilon_G + 1/\varepsilon_S - 1)$ where ε_G is the emmisivity of the oxidant determined by an empirical relationship based on the partial pressure of the water vapor and any carbon dioxide that may be present, the beam length and temperature of the oxidant, and ε_S is the emmisivity of the solid surface taken as 0.9 (Bessette, 1994), h_i is the inside tube convective heat transfer coefficient for fully developed flow.

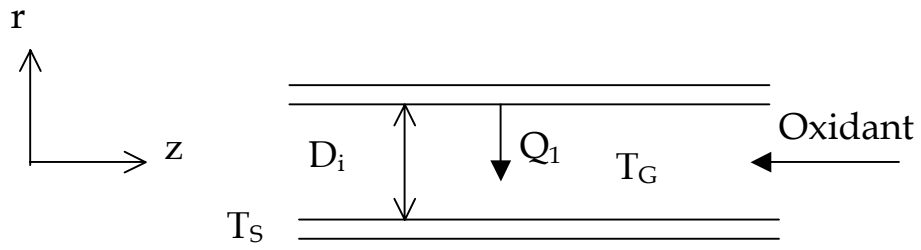

Figure 5. Heat Transfer from the Injector Tube Inside Surface to Oxidant

Equation (2) is integrated over an interval (or zone) Δz by utilizing arithmetic mean temperatures between the inlet and outlet of the preheat zone interval for the convective heat transfer while geometric mean temperatures are used for the radiative heat transfer (Hottel and Sarofim, 1967). Use of the arithmetic means is justified on the assumption that the convective heat transfer rate (which varies along the axial direction) may be adequately expressed by a second order dependence on the axial length (that is, higher order effects may be neglected). Thus $Qc = C_0 + C_1 z + C_2 z^2$, where Qc is the convective heat transfer rate.

The following conditions are substituted into the solution of equation (2):

$$\text{at } z = z_0,\ T_S = T_{Sout},\ T_G = T_{Gout} \quad \textbf{(3)}$$

$$\text{at } z = z,\ T_S = T_{Sin},\ T_G = T_{Gin} \quad \textbf{(4)}$$

where $z - z_0 = \Delta z$, T_{Sin} is the temperature of the solid surface where the oxidant enters the preheat zone interval and T_{Sout} is the temperature of the solid surface at the outlet (where the oxidant leaves the preheat zone interval), T_{Gin} is the temperature of the oxidant as it enters the preheat zone interval, and T_{Gout} is the temperature of the oxidant as it leaves the preheat zone interval. T_{Sout} is assumed = T_{Gout} at z = 0 which is given. The resulting equation then for energy transfer between the inner surface wall of the preheat tube and the oxidant may be expressed as:

$$T_{Sin} = 2[\{Q_1/(\pi D_i \Delta z) - \sigma \varepsilon (T_{S,M}^4 - T_{G,M}^4)\}/h_i + (T_{G,in} + T_{G,out})/2] - T_{Sout} \quad \textbf{(5)}$$

where $T_{S,M}$ and $T_{G,M}$ are the geometric mean temperatures of the solid surface and the oxidant respectively ($T_{G,M}$ is determined from the given oxidant temperature leaving the preheat zone and a trial value assumed for the oxidant temperature entering the preheat zone).

Conduction through Injector (Air Preheat) Tube Wall. Axial symmetry is assumed and heat flux by conduction in the axial direction is assumed constant (that is, temperature is assumed to vary linearly in the axial direction). With these assumptions, the heat transfer equation for a differential element taken in the axial direction (Figure 6): reduces to:

$$dQ_1/dz = 2\pi k (T_{So} - T_{Si})/\ln(D_o/D_i) \quad \textbf{(6)}$$

where T_{So} and T_{Si} are the outer and inner solid surface temperatures, Q_1 is the heat transferred to the oxidant within the air-preheat tube, D_i and D_o are the inside and outside diameters of the injector (air preheat) tube, k is the thermal conductivity of the solid taken as 6.04 W/m K (Bessette, 1994).

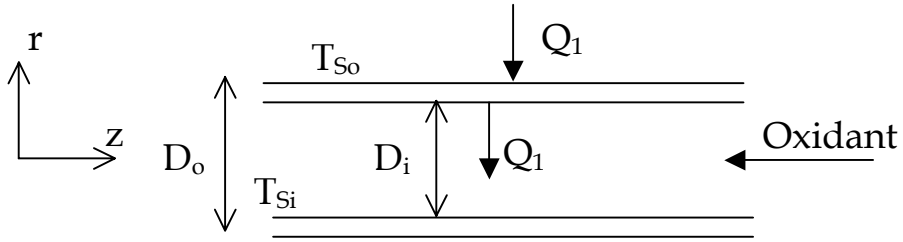

Figure 6. Conduction through Injector (Air Preheat) Tube Wall

Equation (6) is integrated over an interval (or zone) Δz by utilizing arithmetic mean temperatures between the inlet and outlet of the preheat zone interval. Use of the arithmetic means is again justified on the assumption that the heat transfer rate (which varies along the axial direction) may be adequately expressed by a second order dependence on the axial length (that is, higher order effects may be neglected). Thus $Q_1 = a_0 + a_1 z + a_2 z^2$, where Q_1 is the heat transfer rate. The following conditions are substituted into the solution of equation (2):

$$\text{at } z = z_0,\ T_{Si} = T_{Si,out},\ T_{So} = T_{So,out} \qquad \textbf{(7)}$$

$$\text{at } z = z,\ T_{Si} = T_{Si,in},\ T_{So} = T_{So,in} \qquad \textbf{(8)}$$

where $z - z_0 = \Delta z$, $T_{Si,in}$ and $T_{So,in}$ are the temperature of the solid inside and outside surfaces where the oxidant enters the preheat zone interval and $T_{Si,out}$ and $T_{So,out}$ are the temperature of the solid inside and outside surfaces at the outlet (where the oxidant leaves the preheat zone interval) which are assumed = T_{Gout} at z = 0. The resulting equation for conduction through the wall is:

$$T_{So,in} = 2[Q_1 \ln(D_o/D_i)/(2\pi k \Delta z) + (T_{Si,in} + T_{Si,out})/2] - T_{So,ouit} \qquad \textbf{(9)}$$

heat transfer from the Cathode or Substrate Inner Surface to Oxidant and Injector Tube Outer Wall. Both convective and radiant heat transfer in the radial direction are taken into account between the cathode or substrate (if present) inner surface to injector (air preheat) tube outer surface and the oxidant flowing through the annular space, while assuming the oxidant to be a gray gas (Figure 7). Axial symmetry is assumed and heat flux by conduction in the axial direction is neglected in the gas due to its relatively low thermal conductivity. With these assumptions, the radiative and convective heat transfer between the oxidant and the injector outer surface for a differential element taken in the axial direction is given by:

$$dQrc_o/dz = \pi D_o [h_o (T_G - T_{So}) + \sigma F_o (T_G^4 - T_{So}^4)] \qquad \textbf{(10)}$$

where F_o is defined as (Marks' Standard Handbook for Mechanical Engineers, 1996) = $\varepsilon_o \varepsilon_G [1 + D_o/D_i (1 - \varepsilon_G) (1 - \varepsilon_i)]/[1 - \{1 + D_o/D_i (\varepsilon_o \varepsilon_G - \varepsilon_G - \varepsilon_o)\}(1 - \varepsilon_G) (1 - \varepsilon_i)]$ and T_{So} is the outside surface temperature of the injector (air preheat) tube (determined previously), Qrc_o is the radiative and convective heat transfer between the oxidant and the injector outer surface, D_i and D_o are the inside diameter of the substrate or cathode layer and the outside diameter of the injector (air preheat) tube, T_G is mean temperature of the oxidant within the annular space, σ is the Stefan-Boltzmann constant, h_o is the convective heat transfer coefficient between the outside surface of the injector (air preheat) tube and the oxidant, ε_i, ε_o and ε_G are the emmisivities of the cell (cathode or substrate if present) inner solid surface, oxidant, and the air-preheat tube outer solid surface, respectively. The emmisivity of the solid surfaces is taken as 0.9 (Bessette, 1994).

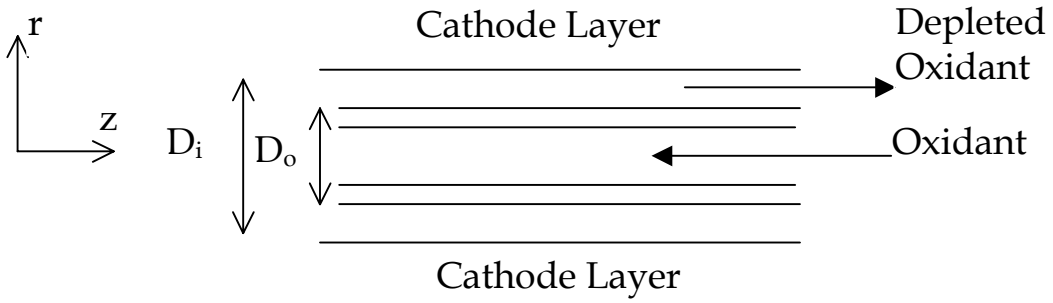

Figure 7. Heat Transfer from the Cathode or Substrate Inner Surface to Oxidant and Injector Tube Outer Wall

The radiative and convective heat transfer between the oxidant and the inside surface of the cathode (or substrate if present) for a differential element taken in the axial direction is given by:

$$dQrc_i/dz = \pi D_i [h_i (T_{Si} - T_G) + \sigma F_i (T_{Si}^4 - T_G^4)] \quad \textbf{(11)}$$

where F_i is defined as (Marks' Standard Handbook for Mechanical Engineers, 1996) $= \varepsilon_i \varepsilon_G [1 + D_o/D_i (1 - \varepsilon_G) (1 - \varepsilon_o)]/[1 - \{1 + D_o/D_i (\varepsilon_o\varepsilon_G - \varepsilon_G - \varepsilon_o)\}(1 - \varepsilon_G) (1 - \varepsilon_i)]$ and T_{Si} is the inside surface temperature of the cathode or substrate if present, Qrc_i is the radiative and convective heat transfer between the cathode or substrate inner surface and the oxidant within the annular space, h_i is the convective heat transfer coefficient between inside surface of the cell (cathode or substrate) and the oxidant. Due to the low mass transfer rate of the oxygen through the cathode, it was determined by applying results presented by Bird el. al. (1960) that the enhancement to the heat transfer coefficient by mass transfer was insignificant.

Next, the radiative heat transfer between the two solid surfaces for a differential element taken in the axial direction is given by:

$$dQr/dz = \pi D_o \sigma F (T_{Si}^4 - T_{So}^4) \quad \textbf{(12)}$$

where F is defined as (Marks' Standard Handbook for Mechanical Engineers, 1996): $= [\varepsilon_o \varepsilon_i (1 - \varepsilon_G)] /[1 - \{1 + D_o/D_i (\varepsilon_o \varepsilon_G - \varepsilon_G - \varepsilon_o)\}(1 - \varepsilon_G) (1 - \varepsilon_i)]$ and Qr is the radiative heat transfer between the two solid surfaces.

The net heat entering the air preheat surface (in the inward radial direction) is then given by:

$$dQ_1 = dQrc_o + dQr \quad \textbf{(13)}$$

and the net heat entering from the cathode or substrate surface (in the inward radial direction) is then given by:

$$dQ_2 = dQrc_i + dQr \quad \textbf{(14)}$$

while an enthalpy balance on the gas side yields

$$dQ_2 - dQ_1 = dH_G \qquad \textbf{(15)}$$

where dH_G is the increase in enthalpy of the oxidant.

Equations (10), (11), and (12) are substituted into equations (13), (14) and (15) and integrated over the length Δz, using arithmetic mean temperature of the oxidant based on its temperature at the inlet and outlet of the tube for the convective heat transfer while geometric mean temperature is used for the radiative heat transfer (Hottel and Sarofim, 1967). Use of the arithmetic mean is justified based on data presented by Bessette (1994) which shows that the gradient in the oxidant temperature is less than 2.5°K per centimeter (cm) in the first half section of a 50 cm long cell while less than 1°K per cm in the second half of the cell (the commercial cells to be offered by Westinghouse will be 150 cm long). Algebraic manipulation of the resulting equations provide the following "working equations":

$$T_{Gout} = 2[(Q_1 - Q_2)/(\pi \Delta z) + \sigma F_i D_i (T_{Si}^4 - T_{G,M}^4) - \sigma F_o D_o (T_{G,M}^4 - T_{So}^4) + D_i h_i T_{Si} + D_o h_o T_{So}]/(D_i h_i + D_o h_o) - T_{Gin} \qquad \textbf{(16)}$$

$$T_{Si} = [T_{So}^4 + \{Q_1/(\pi \sigma D_o \Delta z) - F_o (T_{G,M}^4 - T_{So}^4) - h_o (T_{G,A} - T_{So})/ \sigma\}/F]^{1/4} \qquad \textbf{(17)}$$

where T_{Si} and T_{So} are now defined as the mean inside surface temperature of the cell (substrate or cathode) and outside surface temperature of the injector (air preheat) tube (known from previous step), $T_{G,A}$ and $T_{G,M}$ are the arithmetic and geometric mean temperatures of the oxidant within the annular space respectively.

Heat Transfer in the Substrate, Cathode, Electrolyte and Anode. Both convective heat transfer due to the diffusion of the oxidant through the various layers (substrate if any, cathode and electrolyte) of the cell and conduction of heat through the layers is taken into account in the radial direction (Figure 8). Similarly the heat transfer due to passage of H_2 and H_2O through the anode is taken into account. Temperature of the gas is assumed to be the same as temperature of the solid at a given point. Again heat flux by conduction in the axial direction is assumed constant while conduction in the gas phase is neglected due to its relatively low thermal conductivity.

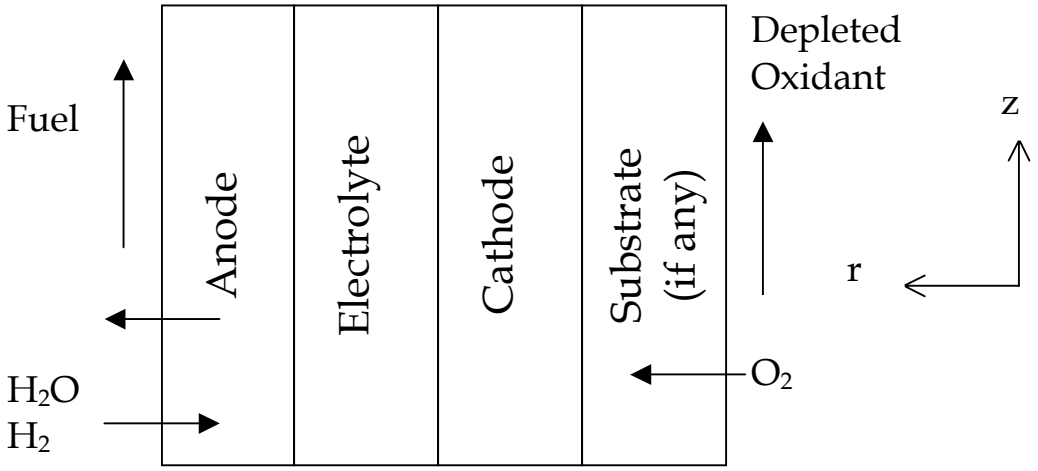

Figure 8. Heat Transfer in the Substrate, Cathode, Electrolyte, and Anode

With these assumptions, the continuity equation when applied to the oxidant diffusing through the solid in the radial direction is given by:

$$d(\rho r v_r)/dr = 0 \qquad \textbf{(18)}$$

where ρ is the density and v_r is the radial superficial velocity of the oxidant. The energy equation applied to the oxidant and the solid with the above assumptions is given by:

$$\rho C_P v_r \, dT/dr - k\,[(1/r)\, d(r\, dT/dr)/dr] = q_{gen} \qquad \textbf{(19)}$$

where T is the oxidant or solid temperature, q_{gen} is the heat generated within the layer per unit volume (determined from the irreversibilities within the cell as explained later), C_P is the specific heat of the diffusing oxidant, k is the bulk thermal conductivity of the solid layer.

Equations (18) and (19) are integrated over a single solid layer in the radial direction assuming axial symmetry and applying the following boundary conditions:

at $r = r_i$, $T = T_i$, $dT/dr = q_{trans}/k$ (both quantities previously determined),

at $r = r_o$, $T = T_o$ (to be determined),

where r_i and r_o are the inside and outside radii of the layer and q_{trans} is the conductive heat transfer flux through the layer at its inner surface in the radial direction. The resulting working equation obtained for a given layer of the cell assuming that the heat generated within a given layer is uniformly distributed within that layer:

$$T_o = T_i + D_i/(2\,k\,\Delta z)\left[-Q_{gen}\,D_i\,\{(D_o/D_i)^2 - 1\}/\{(D_0^2 - D_i^2)(2-\alpha)\}\right.$$
$$\left. + [2\,Q_{gen}\,D_i/\{(D_0^2 - D_i^2)(2-\alpha)\} + Q_{trans}/(D_i\,\alpha)]\{(D_o/D_i)^{\alpha} - 1\}\right] \quad \textbf{(20)}$$

where T_o and T_i are now defined as the mean temperatures for a zone (of length Δz in the axial direction) at its outer and inner surfaces, Q_{gen} is the total heat generated within the layer, Q_{trans} is the total heat transferred through the layer at its inner surface in the inward radial direction, D_i and D_o are the inside and outside diameters of the layer, $\alpha = C_P\,m_{O2}/(k\,\Delta z)$, m_{O2} is the oxidant mass flow rate.

Equation (20) is applied to the inner most layer (substrate layer if present and then to the cathode layer) where its inside surface temperature T_i and the heat flux across this surface are known from the previous step.

Heat transfer within the electrolyte layer and the anode layer are similarly modeled.

Heat Transfer between Fuel and Anode. Both convective and radiant heat transfer in the radial direction are taken into account between the fuel and the outside surface of the anode layer (Figure 9).

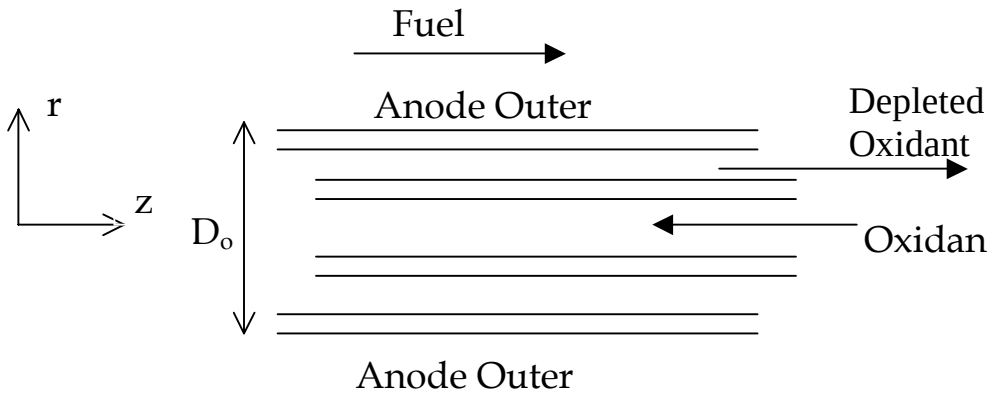

Figure 9. Heat Transfer between Fuel and Anode

Again conduction in the axial direction is neglected. With this assumptions, the heat transfer equation for a differential element taken in the axial direction reduces to:

$$dQ/dz = (\pi - \theta)\,D_o\,[h_o\,(T_G - T_S) + \sigma\,\varepsilon\,(T_G^4 - T_S^4)] \quad \textbf{(21)}$$

where Q is the net heat transferred to the anode (determined by an enthalpy balance, $dQ = dH_G$, where dH_G is the change in enthalpy of the fuel), θ is due to the interconnect between adjacent tubes, T_S is the temperature of the outside solid surface, T_G is the temperature of gas (fuel), D_o is the outside diameter of the anode layer, σ is the Stefan-Boltzmann constant, $\varepsilon = 1/(1/\varepsilon_G + 1/\varepsilon_S - 1)$ where ε_G is the emmisivity of the fuel determined by an empirical relationship based on the

partial pressure of the water vapor, carbon dioxide, carbon monoxide and methane present, the beam length and temperature of the fuel, and ε_S is the emmisivity of the solid surface taken as 0.9, h_o is the convective heat transfer coefficient.

Equation (21) is integrated over an interval (or zone) Δz by utilizing arithmetic mean temperatures between the inlet and outlet of the interval for the convective heat transfer while geometric mean temperatures are used for the radiative heat transfer (Hottel and Sarofim, 1967). Arithmetic mean temperature for the fuel based on its temperature at the inlet and outlet of the tube is used for the convective heat transfer while geometric mean temperature is used for the radiative heat transfer. Use of the arithmetic mean is justified based on data presented by Bessette (1994) who shows that the gradient in the fuel temperature is less than 0.5 ^oK per cm in 90 percent of the cell (at the entrance, the fuel is heated from its initial temperature to the cell temperature within 5 cm of length). The following conditions are substituted into the solution of equation (21):

$$\text{at } z = z_0,\ T_G = T_{Gin} \qquad \textbf{(22)}$$

$$\text{at } z = z,\ T_G = T_{Gout} \qquad \textbf{(23)}$$

where $z - z_0 = \Delta z$. The resulting equation then for energy transfer between the inner surface wall of the preheat tube and the oxidant may be expressed as:

$$T_{Gout} = 2\left[\left[Q/\{(\pi - \theta)D_o\Delta z\} - \sigma\varepsilon\,(T_{G,M}{}^4 - T_{So}{}^4)\right]/h_o + T_{So}\right] - T_{Gin} \qquad \textbf{(24)}$$

where T_{So} is now defined as the mean temperature of the anode outer surface determined previously.

2.4.2.2 Mass Transfer

Mass transfer of the oxidant consists of convective transfer to the substrate wall (if any) or the cathode from the bulk gas, followed by diffusion within the pores of the cathode, surface adsorption at the pore walls and diffusion through the solid. The mass transfer equation with the associated resistance of each of these transfer modes for a difference element of the tube taken in the axial direction (for the case without a substrate layer which is the current approach being taken by the tubular SOFC manufacturers) for a given ratio of actual current density (i) to limiting current density (i_L) is given by:

$$M_{O2} = (i/i_L)C_{O2}/$$
$$\left[1/(\pi D_i k_x \Delta z) + [m_1 D_o \ln(D_o/D_i)/(2m_2 m_3) + \tanh(mL)/(Kmm_3)]/[1 - 1/\cosh(mL)]\right] \qquad \textbf{(25)}$$

where:

$$m_1 = 2\,k_s\tau_g/(D_g\,r_p)$$

$$m_2 = 2\,\varepsilon\, k_s \tau_s / [(1-\varepsilon) D_s\, r_p]$$

$$m = \sqrt{(K m_1 + m_2)}$$

$$m_3 = (1-\varepsilon)\,\pi\, D_o\, \Delta z\, D_s$$

$$L = (D_o - D_i)/2$$

τ_g is an empirically determined factor to account for deviations from the ideal pore assumption, that is, to account for (i) the gas phase tortuosity which is defined as the ratio of the actual distance a molecule travels between two points to the shortest distance between those two points and (ii) the variability of the pore diameter. τ_s is the solid phase tortuosity. Adler et al. (1996) report a value of $\tau_g = 1.5$ based on scanning electron microscopy measurements of a similar perovskite ($La_{0.6}Sr_{0.4}Co_{0.2}Fe_{0.8}O_{3-\delta}$) sample while Deng et al (1994) estimate a value of τ_s =1.16. K is the equilibrium constant between the solid phase and the gas phase oxygen concentrations. ε is the porosity of the cathode assumed 50 percent (data presented in the International Energy Agency Report tilted "Facts and Figures," 1992 gives a range of 35 to 60 percent). r_p is the pore radius estimated at 0.017 μm corresponding to a porosity of 50 percent from the data presented by Sasaki, 1996 for the specific internal surface area of 9 m^2/g for the cathode prepared by calcining the powder at a temperature of 800°C. C_{O2} is the concentrations of oxygen in the bulk gas. D_i and D_o are the inside and outside diameters of the cathode layer. Equation (25) represents a simplified form (of the more general solution that was derived which included modified Bessel functions of zero order) for the special case where the thickness of the cathode layer (L) is small in comparison to the diameter of the tube and where the value of mL is large.

In equation (25) (which represents the diffusion rate over an interval or zone Δz), arithmetic mean for the concentration is used based on the inlet and outlet concentrations of the oxygen in the bulk gas. Use of the arithmetic mean is justified on the assumption that the mass transfer rate (which varies along the axial direction) may be adequately expressed by a second order dependence on the axial length (that is, higher order effects may be neglected).

The solution technique for determining the overall cell voltage consists of varying the ratio i/i_L rather than varying the absolute value of i. Thus equation (25) is in a convenient from for determining the oxygen transport rate for a desired cell voltage.

The surface exchange coefficient and the diffusion coefficient through the solid are given by the following relationships based on data presented by Lane et al. (1995), Elshof et al. (1997) and Belzner et al. (1992):

$$k_s = 105.6 \times 10^{-6}\, (P_{O2})^{.745}\, \exp[-25{,}688/(RT)] \qquad \textbf{(26)}$$

$$D_s = 4.499 \times 10^{-3}\, (P_{O2})^{.2957}\, \exp[-38{,}223/(RT)] \qquad \textbf{(27)}$$

where P_{O2} is the partial pressure of oxygen in atmosphere (atm), R is the universal gas constant (= 1.987 cal/g mole °K) and T is the absolute temperature, k_s is in m/s and D_s is in m^2/s.

The rate limiting step of charge transfer on the anode side has been identified experimentally to be the diffusion of the H_2 through the boundary layer between the fuel and the anode at the outside anode surface and not the diffusion of the H_2 through the pores by Primdahl and Mogensen (1999). Furthermore, under practical operating conditions of the SOFC where high steam to carbon ratios are maintained in the fuel gas to avoid carbon deposition in the anode, direct oxidation of the CO and CH_4 is insignificant as shown experimentally by Matsuzaki and Yasuda (2000), and Park et al. (1999) and Ihara et al. (1999).

Thus, it is the H_2 that takes part in the anode electrochemical reaction, its concentration at the fuel/anode interface being determined from the following relationship:

$$M_{H2} = k_x (\pi - \theta) D'_o \Delta z (C_{H2} - C'_{H2}) \quad \textbf{(28)}$$

while that of the formed H_2O is given by:

$$M_{H2O} = k_{x,\,H2O} (\pi - \theta) D'_o \Delta z (C_{H2O} - C'_{H2O}) \quad \textbf{(29)}$$

From stoichiometry of the H_2 oxidation reaction:

$$M_{H2} = -M_{H2O} \text{ and } M_{H2} = 2\, M_{O2} \quad \textbf{(30)}$$

θ is due to the interconnect between adjacent tubes, M_{H2} and M_{H2O} are the molar rates of transfer of H_2 to the anode outer surface and of transfer of H_2O from the anode surface, C_{H2} and C_{H2} are the bulk concentrations of H_2 and H_2O in the gas phase, C'_{H2} and C'_{H2O} are the concentrations of the H_2 and H_2O in the gas phase at the anode/gas interface, k_x is the specie mass transfer coefficient, and D'_o is the outside diameter of the anode.

For fuel mixtures containing CO without H_2 and H_2O such that the shift reaction cannot occur and the direct oxidation of CO occurs, equations involving CO and CO_2 are analogously written. As pointed out previously, however, practical SOFC applications do not use such fuels to avoid carbon deposition within the anode.

2.4.2.3 Heat Generation

The maximum power that may be developed by the cell is given by the Gibbs free energy change for the oxidation reaction of the fuel. However, the irreversiblities within the cell limit the conversion to useful work. The irreversiblities consist of concentration polarizations caused by a build up of reactants or products at the electrodes, activation polarizations that are caused by the non-equilibrium nature of the actual electrochemical reactions, the ohmic losses, and those due to entropy change of the reactions. The voltage drops due to each of these irreversiblities are given by the following relationships.

Concentration Polarization. Concentration Polarization that occurs in the cathode is given by (Hirschenhofer et al. 1994):

$$\eta_C = RT/(2F) \ln(1 - i/i_L) \quad \textbf{(31)}$$

where η_C is the voltage drop, R the universal gas constant, T is the absolute temperature, F is Faraday's constant and i_L is the limiting current density in the cathode (the ratio i/i_L on the cathode side is determined iteratively to obtain the desired voltage). The concentration polarization on the anode side is similarly determined.

Activation Polarization. Activation Polarization that occurs both in the cathode and the anode is obtained from:

$$\eta_A = RT/(2F)\ \ln(i/i_o) \qquad \textbf{(32)}$$

where η_A is the voltage drop, R the universal gas constant, T is the absolute temperature, F is Faraday's constant, i is the current density, i_o is the exchange current density which is a function of temperature for a given material determined for the cathode and anode from data presented by Divisek et al., (1994) and Kim et al., (1999), respectively. The correlation developed by Divisek et al., (1994) for the pressure dependence of the cathode exchange current density of the form $i_o \propto (p_{O2})^{0.83}$ is used.

Ohmic losses. Ohmic losses occur due to the electrical resistance to the flow of electron or ionic species. Figure 10 depicts the electron path through the cathode, the oxygen ion path through the electrolyte and electron path through the anode. The oxygen ion path through the cathode is assumed to be in the radial direction. The current enters the cathode on one side of the tube and leaves the anode on the other side.

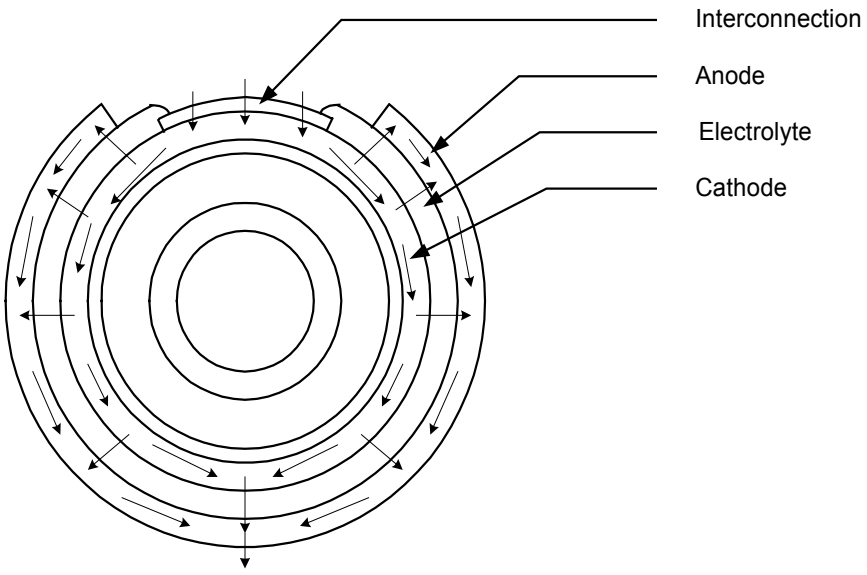

Figure 10. Electron/Ionic Flow Path

Thus, for the cathode and anode layers, the electric path for determining the resistance is taken as half of the total length in the circumferential direction. Its justification is based in the assumption that the electron flux at the entrance of the cathode or at the exit of the anode which is in the circumferential direction is uniform in that direction while the oxidant and fuel flow uniformly in the radial direction in the cathode and anode respectively (the gas and the electron

paths before the electrons interact with the oxidant in the case of the cathode, and after they are liberated from the oxygen ions in case of the anode are normal to each other).

The electrical resistivity for each of the layers is taken from Fee, Zwick, and Ackerman (1983). The current flow through the anode or cathode is taken as half the total since the current distributes itself equally between the two semi-circular paths. The heat generated due to these irreversiblities is given by the product of the voltage and the current.

In addition to the heat generated by the irreversiblities due to the cell polarizations, the cell generates heat due to the entropy change of the reaction at the cathode where the oxygen molecule is converted to an ion and absorbs heat due to the entropy change of the reaction at the anode where the fuel is oxidized by the oxygen ion.

The heat generated at the cathode is determined (by the product of the absolute mean temperature in the cathode layer and the entropy generated in the cathode) for the electrochemical reaction with the molecular oxygen present at a partial pressure corresponding to that in the gas bulk:

$$1/2\ O_2 + 2e^- = O^= \qquad \textbf{(33)}$$

The heat absorbed in the anode is calculated by subtracting the above heat generated due to entropy change at the cathode from the total heat generated due to the entropy change of the overall oxidation reaction of the fuel (H_2) with the molecular oxygen at the gas bulk partial pressure (for fuel mixtures containing CO without H_2 or H_2O the entropy change of CO oxidation is used). Partial pressure corresponding to that in the bulk gas are also used for H_2 and H_2O (or CO and CO_2). The temperature of the anode is used in calculating the overall heat generation (the temperature difference between the anode and the cathode is less than 3°K). Note that the concentration polarization corrects for the actual partial pressures of the O_2, H_2 and H_2O at the electrode, which are different from the gas bulk.

2.4.3 Solution strategy

The solution strategy consists of starting the calculations at the "bottom" of the cell where the oxidant leaves the preheat tube and enters the annular space between the cathode and the preheat tube. For a given set of temperatures for the oxidant and the fuel at this cross-section (initial conditions), a temperature drop for the air inside the preheat tube and the ratio of actual current flow to the limiting current flow are assumed. The heat and mass transfer equations defined previously are solved from section to section in the radial direction. Each of the heat generation terms due to the irreversiblities and the entropy changes is used in equation (20). The net DC electric power generated is calculated by subtracting the total heat generated due to the irreversibilities including those due to entropy changes of the cathode and anode reactions, from the overall enthalpy change for the oxidation reaction of the fuel with molecular oxygen. Next, an energy balance is made and the assumed temperature drop of the air inside the preheat tube is adjusted accordingly. Thus a solution is arrived at iteratively and the resulting voltage is calculated from the power produced and the current flow. Iterations are continued if the voltage calculated does not match the desired voltage by adjusting the ratio of actual current flow to the limiting current flow and repeating the entire iterative process defined above. The

depleted oxidant and fuel finally exit the SOFC module; the depleted fuel may be combusted by the depleted oxidant if desired utilizing the combustor module.

The procedure for solving the heat and mass transfer and the electrochemical processes consists of:

1) Starting at the bottom of the SOFC that is, at the end opposite to the feed end
2) And assuming a temperature decrement on the air side (preheat section)
3) Solving for the temperature profile, oxygen transport and the electrochemistry in the radial direction
4) Check if the voltage calculated matches the voltage specified for the cell
5) Iterate to Step 2 as required

The depleted fuel is combusted with the depleted oxidant and the incoming air and fuel absorb a portion of the heat released. Note that the fuel is also reformed in this section, and the heat released by the combustion of the depleted fuel also supplies the endothermic heat required by the reforming process.

The user may specify the fuel composition (H_2, H_2O, CO and CH_4), air temperature and fuel temperature entering the SOFC module, the operating pressure and the cell diameter. An estimate of the power required and the heat rate is required as part of the input.

The module calculates the current density, the length of each tube, number of tubes, thermal efficiency and the exhaust conditions. A working copy of this module has been delivered with previous reports and is also included in the submission of this final report.

The current module models the thermodynamics of a tubular solid oxide fuel cell, one of the most promising and robust SOFC designs. The model consists of solving the heat and mass transfer equations in the radial direction while assuming chemical reaction equilibrium in the anode section. Heat and mass transfer in the axial direction are neglected. This is a reasonable assumption since the unit is nearly isothermal along the length of the fuel cell and the mass transfer is dominated by convection in the axial direction.

2.5 Related Research and Discussion

Dunbar and Gaggioli developed a purely thermodynamic model for an SOFC and neglected the important rate controlling processes such as the conduction of heat through the solid and the mass transfer of the oxidant. Wepfer and Woolsey (1985) modeled the SOFC with the assumption that the system remains isothermal and also neglected the heat transfer effects. Kanamura et al. (1989) took into account the non-isothermal behavior of the tubular SOFC but neglected the concentration polarization effects. Furthermore, these three models are limited to pure hydrogen/water vapor mixtures as the fuel and none of these models takes into account the rate limiting electrochemical transfer of the oxygen through the cathode.

Bessette (1994) developed a model for the tubular SOFC consisting of finite element analysis using the commercially available ANYSYS computer program. The tubular SOFC model takes into account most modes of heat transfer within the cell. The mass transfer resistance through

the cathode was again not taken into account while diffusion through the porous cathode-support tube (which is not used in the today's SOFCs) was modeled as diffusive mass transfer through a film of gas of thickness equal to the physical thickness of the support tube. The tortuous path for gas diffusion through the porous cathode due to the pores, the surface adsorption and the rate controlling step of diffusion through the solid were not accounted for. Furthermore, the fuel constituents were not allowed to react with each other (carbon monoxide present in the anode gas was not allowed to undergo the shift reaction). Radiation from the fuel and its products of oxidation was also neglected. The heat transfer associated with the oxygen diffusing through the cell to react with the fuel was neglected as was done by the other authors cited above.

Haynes (1999) developed a model similar to that developed by Bessette and furthermore neglected the activation polarization. The shift reaction was however, taken into account in the anode section of the cell.

Table 2 summarizes the assumptions made in this study and those made by the previous authors. A model that fully integrates the heat and mass transfer processes with the electrochemical processes occurring within the SOFC has not been reported in literature.

Table 2. SOFC Model Assumptions

	Kanamura et al. (1989)	Bessette (1996)	Haynes (1999)	This Study
Type of Model	Finite element analyses while assuming axial symmetry	Finite element analysis (ANYSYS)	Finite element analysis	Integral (use of mean potentials for transfer processes)
Heat Transfer	Neglected anode heat transfer, due to oxygen diffusion & radiation	Neglected anode surface/gas radiation, neglected heat transfer due to oxygen diffusion	Neglected anode & gas radiation, neglected heat transfer due to oxygen diffusion	Constant axial heat flux for conduction through solid
Cathode Mass Transfer	Neglected	Pore/solid diffusion & adsorption of O2 not included	Does not provide explanation on how this process is modeled	Pore diffusion & adsorption of O2 taken into account
Cell Irreversibilities	Neglected concentration polarization	Attempted to include significant ones	Neglected activation polarization	Included all significant ones
Fuel	H_2/H_2O mixtures	H_2, CO, CH_4 (Frozen Chemistry)	H_2, CO, CH_4 (Shift reaction equilibria)	H_2, CO, CH_4 (Shift reaction equilibria)

2.5.1 SOFC Hybrid System Analysis

Existing models for analysis of systems such as power cycles may be divided into two types: (1) those developed for simulating chemical process plants (e.g. commercially available Hysis, Aspen, Pro II) and (2) those developed for simulating power plants (e.g. commercially available ThermoFlex and GATE/Cycle). Models in the first category have the capability for predicting the thermodynamic properties of non-ideal systems but do not include the proper models for power cycle equipment such as gas turbines, steam turbines and fuel cells. The models in the second category have the capability of modeling gas and steam turbines but not fuel cells nor the capability of predicting the properties of non-ideal gases except for pure steam. Thus these models for example, cannot predict the Joule-Thompson cooling of natural gas when its pressure is reduced from typical pipeline pressure (50 bar) to the pressure required by a heavy frame gas turbine that typically operates at a pressure-ratio in the neighborhood of 15.

Furthermore, with greenhouse gas emissions becoming a more global concern, the recovery and compression of the carbon dioxide to supercritical pressures, which is typically required for disposal, is becoming a requirement in many advanced cycle analysis programs, requiring the capability of predicting the non-ideal behavior of carbon dioxide.

Models in the second category do not include modules for simulating reactors such as a shift reactor in cases where CO_2 removal and capture or production of H_2 for a phosphoric acid fuel cell (PAFC) or proton exchange membrane fuel cell (PEMFC) is required. Simplified models are included for counter-current multi-stage humidification which is being incorporated into advanced Brayton type of power cycles consisting of evaporating water into the working fluid, and partial oxidation reactor to convert a fuel such as coal or heavy fuel oil into synthesis gas suitable as fuel to a fuel cell.

Models for simulating fuel cell based plants have been developed by Ferguson (1989), Bessette (1994), and Haynes (1999) but these models are limited to systems consisting of ideal gases and pure steam in addition to the limited theoretical depth of the SOFC models. Furthermore, the models required for simulating many of the unit operations and processes that could make-up a hybrid plant are not included such as a gas turbine that accounts for the cooling load of the blades, a counter-current multi-stage humidifier, and a partial oxidation reactor.

The counter-current humidifier is being incorporated in advanced cycles in order to recover low temperature waste heat and use it for the evaporation of water into the gaseous fuel or air under pressure to increase the amount of working fluid. The equations governing the simultaneous heat and mass transfer occurring within a multistage counter-current column have been presented by various authors such as Kern (1950), McCabe and Smith (1976), Foust et al. (1980) and Enick et al. (1994). The heat transfer between the water and the gas due to the sensible heat carried by the diffusing water vapor was not included by any of these authors. This results in as much as 10 percent of the total energy transferred being unaccounted for in cases where humidification to an extent of 0.2 to 0.3 kg of water vapor per kg of gas is accomplished within the humidifier.

Thus in addition to a model for the SOFC, a need exists for a system model suitable for the analysis of SOFC based hybrid cycles. The analysis capability required includes an analytical model for the tubular SOFC as well as the secondary equipment required to analyze a hybrid power plant such as a gas turbine, reformer or partial oxidation reactor, shift reactor,

humidifier, steam turbines, compressor, gas expander, heat exchangers and pump. In addition to these equipment models, modules for functions such as separating a component from a stream or splitting a stream or combining streams and Solver to automatically iterate in order to meet the desired process or system design criteria such as maintaining a specified steam to carbon ratio in the reformer feed stream or a specified temperature difference between two streams are required. Another important requirement is the capability to arrange the various components or modules as defined by the user in order to configure different hybrid systems.

Table 3 summarizes the major features and capabilities of available system models relevant to SOFC hybrid analysis and those developed by this study.

Table 3. Major Features of SOFC Hybrid System Models

	Ferguson (1989)	Bessette (1996)	Haynes (2000)	This Study
Thermodynamic basis for Stream Properties	Limited to ideal gases, steam & single phases	Limited to ideal gases, steam & single phases	Limited to ideal gases, steam & single phases	Non-ideality taken into account. Gas-water phases in equilibrium are handled
SOFC Model	Major simplifications	Simplifications	Major simplifications	Takes into account electrochemistry and associated transport processes more thoroughly
Gas Turbine Model	Simplified	None	Simplified	Takes into account blade cooling requirements
Humidifier Model	None	None	None	Transport based model (simultaneous heat & mass transfer)
Reactors	Only reformer	Only reformer	Reformer and shift	Reformer, shift and partial oxidation

2.5.2 SOFC Hybrid Cycle

The next challenge in the area of fuel cell based hybrid systems remains in identifying cycle configurations that have high thermal efficiency and also have attractive cost of electricity. Cost of electricity is a function of the plant thermal efficiency as well as a function of the plant cost, while the plant cost is generally reduced when the configured system is simplified. Simplicity also lends ease to the controllability of the plant, which is a major issue for a plant that sees various operating modes as a result of varying power output demand as well as varying ambient conditions.

Hybrid cycles have been proposed in the past, such as that proposed by Westinghouse (Bevc and Parker, 1995) and described previously as the SureCell™ hybrid which combines a tubular SOFC with an intercooled reheat gas turbine where the SOFC exhaust is introduced into the HP combustor of the gas turbine. A disadvantage with this cycle is that significant amount of heat is rejected from the cycle to the environment (the intercooler heat is all rejected to the atmosphere as well as the stack temperature is high). This hybrid configuration however, does show the most simplicity when compared to hybrid cycle configurations as proposed by others.

The other cycle configurations as proposed for fuel cell based hybrid plants and described in the following have the disadvantage of being very complex and thus are not being proposed for

inclusion in any of the fuel cell based plants currently being built or those that are being designed.

Shingai et al. (1989) disclosed a high pressure fuel cell/gas turbine based hybrid system and a method for operating the system. Natural gas is fed to an external reformer and the reformed fuel is then fed to the fuel cell. Combustion of the depleted fuel or the anode gas from the fuel cell that consists of the partially oxidized fuel provides heat for the endothermic reactions occurring within the reformer. The products of combustion along with the excess oxygen contained in this stream are fed to the gas turbine combustor as vitiated air after being cooled in the reformer. This system configuration which requires the addition of an external reformer not only complicates the configuration which tends to increase the plant cost but also consists of exchanging heat between an oxygen containing gas and a combustible gas. Potential for leakage through the heat exchange equipment precludes the practical application of this system.

Levy et al. (1989) disclosed an apparatus for fuel reforming in a fog cooled fuel cell power plant assembly. Methane is reformed and then supplied to the anode of a fuel cell along with a water fog as a coolant. The anode exhaust stream is divided and supplied to the reformer burner and reformer. The products of combustion leaving the reformer along with gases leaving the cathode are supplied to a gas turbine. In this system a portion of the high temperature heat rejected by the fuel cell is used for vaporization of the fog. Vaporization of the fog in this manner is an inefficient use of the high temperature heat rejected by the fuel cell.

Cohen et al. disclosed a concept consisting of a fuel cell power plant that can be operated at high reactant pressures for improved operation. Twenty percent of the fuel entering the plant is diverted to a boiler that produces steam to operate a steam turbine that turns a compressor to supply air to the cathode of the fuel cell. The remaining 80 percent of the fuel is supplied to a reformer that in turn supplies fuel to the anode of the fuel cell. The exhaust from the cathode and anode are supplied to a burner in the reformer. Steam is used as a coolant in the fuel cell where the steam is superheated. The superheated steam is then used in a turbine to generate additional electric power. This cycle is not only complex in that it adds a Rankine cycle to the system but also is inherently inefficient since a significant portion of the fuel energy is fed directly to the bottoming Rankine cycle.

2.5.3 Summary of Related Research

The emergence of fuel cell systems and hybrid fuel cell systems requires the evolution of analysis strategy for evaluating thermodynamic performance and directing design and development. Related research has been presented and discussed in this section. This section presents some summary statements in light of this related research and the current work.

The present research objective is directed to developing the analysis tools for the evaluation of the SOFC fuel cell systems and SOFC hybrid systems performance, and the identification of promising hybrid systems that maintain high thermal efficiency and potentially lower the cost of electricity. To meet the current research objective, several advances are required compared to approaches available in the literature.

The SOFC model should account for the heat and mass transfer processes occurring within the cell as well as the electrochemistry such that the calculated performance reflects the particular

system design conditions such as fuel composition, operating pressure, fuel utilization and geometric parameters such as tube dimensions.

The gas turbine model should account for changes in the cycle design conditions such as operating pressure, turbine firing temperature, and fuel and oxidant temperature and composition. The gas turbine model should be able to adjust the required turbine cooling flows or the firing temperature to correspond to changes in the temperature or composition of the working fluid or coolant. These changes should be based on the effective technology parameters derived from the gas turbine manufacturer's published data, in order to stay within the constraints of the maximum blade metal temperature.

The humidifier model should account for the simultaneous heat and mass transfer processes. The remainder of the equipment can be modeled on a thermodynamic basis directly consistent with that available in the literature.

An equation of state capable of estimating the enthalpy and entropy corrections for non-ideality of the gas streams is required in order to handle highly non-ideal streams such as natural gas at pipeline pressures, and supercritical CO_2. A separate property package for steam and water is required (derived from the ASME steam tables) including correction for the enthalpy of water due to pressure above its saturation pressure.

Finally, the identification of hybrid cycle configuration is required that converts efficiently and cost effectively the fuel-bound energy that is not converted by the fuel cell to power due to the cell irreversibilities. These irreversibilities are associated with (1) heating of the reactants to the reaction temperature, (2) cooling of the products from the reaction temperature, (3) the entropy change of the reaction, and (4) the cell polarizations. Properly configuring hybrid cycle(s) to maximize the overall system efficiency remains to be a technological challenge due to these and other issues.

2.6 SOFC Module Results

Preliminary results from the SOFC module developed in this project are presented in Figure 11. Results from the module are presented in Figure 11 compared to the measured performance of a Siemens Westinghouse Power Corporation (SWPC) tube bundle as operated at various pressures.

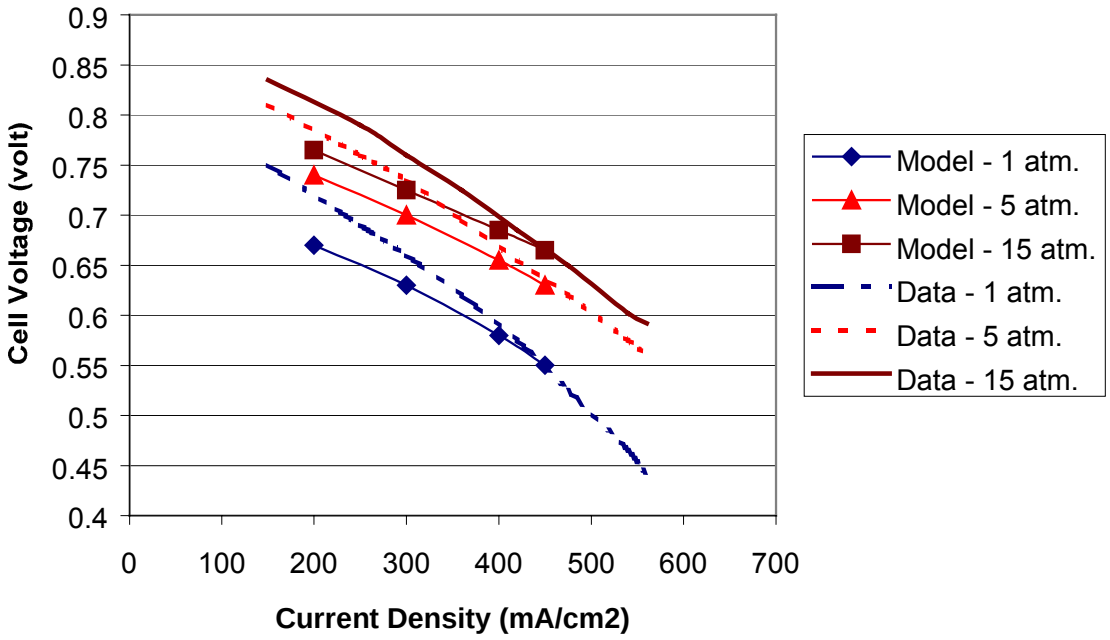

Figure 11. Energy Steady Sim Results – Comparison to SWPC Data tube bundle at various operating pressures

Note: SWPC data are presented as solid lines and model results are presented as lines plus symbols.

No parameters were adjusted in the simulation to bring the simulation results into agreement with the data. In addition, the exact conditions of the SWPC tests, including the dimensions of the cells (which is proprietary information), and details regarding material properties and heat transfer to the environment and amongst the cells (including heat transfer properties of the materials (materials are proprietary and properties are unknown) were not known. Nonetheless, the comparison shows that the current SOFC simulation module well captures the effect of pressure and matches quantitatively well for high current densities. The model shows a logarithmic dependence of fuel cell performance on pressure. At lower current densities the predicted cell voltage is lower than that measured. This may be due to one of the electrochemical loss (over potential) calculations in the model or any of the unknown conditions. Future efforts can address this problem if it is deemed necessary. Overall the SOFC module prediction well matches both the trend and magnitude of the observed data.

2.7 Reformer Simulation Module

A computer simulation module was developed and tested for analysis of a natural gas reformer. The module performs a thermodynamic analysis of natural gas reformation technology, which can be integrated with and used for a variety of fuel cell and fuel cell hybrid systems designs. Variations in operating parameters, fuel and oxidant properties, and operating conditions can be accomplished with the module. Included in the analysis module is a DOS-based user interface that allows ready modification of thermodynamic properties, design parameters and conditions of interest.

Development of a reformer model was required since the differences between natural gas reformation processes accomplished in refinery applications, for example, are very different from those associated with the SOFC and SOFC hybrid systems. Software that is available or reported in the literature for natural gas reformation processes typically can model large hydrogen generation plants used for refinery, hydrogenation and other industrial processes. These systems, however, differ significantly from those contained in an SOFC system. First, the reformer used in a fuel cell hybrid system is typically integrated thermally into the fuel cell stack system to accomplish heat transfer from the stack to the reformer. This transfer of heat is accomplished at temperatures much lower than that associated with a typical reformer which uses direct firing (combustion) of natural gas to overcome the endothermicity of the reformation reactions. Second, the reformer in an SOFC system could also receive fuel cell stack anode off-gas and an input to supply the water (steam) required to accomplish the steam reformation chemical reactions. This anode off-gas typically contains many constituents other than steam which make the process much different than that associated with a typical steam reformation process. Third, the reformer used in an SOFC system only accomplishes a partial reformation of the natural gas to a hydrogen rich mixture. Fourth, the reformer used in an SOFC system does not contain the typical high temperature shift (HTS), low temperature shift (LTS), CO polishing reactor, and pressure swing absorption (PSA) systems that are present to produce a pure hydrogen stream in the typical steam reformation system.

2.7.1 Reformer Model

The reformer module is the second key module that has been developed for the simulation of a hybrid fuel cell gas turbine system. The module calculates the thermodynamics of a natural gas reformer. The model consists of solving the heat and mass transfer equations that govern a counter-flow packed bed reformer. The reformation process occurs as natural gas is introduced into a packed bed of steam reformation catalyst along with a sufficient amount of heat and steam as that contained in a typical exhaust of an operating solid oxide fuel cell (SOFC). This allows the simulation of the design of a Siemens Westinghouse Power Corporation tubular SOFC with integrated reformer as well as other designs that contain steam reformation processes for converting hydrocarbon fuels to carbon monoxide and hydrogen mixtures. Other examples of this include the direct internal reformation process of FuelCell Energy Corporation and the indirect reformation process of many other manufacturers (e.g., ONSI).

The reformer module calculates the effluent composition and conditions for a given set of design parameters such as the feed composition and conditions of pressure and temperature, pressure drop through the reactor, and the required heat transfer rate for a desired outlet temperature.

These calculations are made by solving a set of simultaneous equations consisting of the elemental balances, energy balance and the reaction quotients that represent the approach to equilibrium at the outlet conditions of the reactor. The approach to equilibrium is determined by specifying the difference in the actual bulk temperature of the reactor effluent and the temperature used in calculating the chemical equilibrium constant for each of the thermodynamically independent reactions (this methodology is the standard industry practice). This chemical equilibrium constant then becomes the reaction quotient corresponding to the actual conditions prevailing in the reactor effluent. Thus, for an incomplete exothermic reaction, the temperature used in calculating the equilibrium constant is specified higher than the actual reactor effluent temperature, while for an incomplete endothermic reaction, the temperature used in calculating the equilibrium constant is specified lower than the actual reactor effluent temperature.

The thermodynamically independent reactions are:

$$CO + H_2O = H_2 + CO_2 \quad \textbf{(34)}$$

$$CH_4 + H_2O = 3H_2 + CO \quad \textbf{(35)}$$

The equations that describe the performance of a reformer include the following elemental balances:

H_2 balance:

$$2m_{CH4} + m_{H2} + m_{H2O} = M_{H2} \quad \textbf{(36)}$$

C balance:

$$m_{CH4} + m_{CO} + m_{CO2} = M_C \quad \textbf{(37)}$$

O_2 balance:

$$0.5\, m_{CO} + m_{CO2} + 0.5 m_{H2O} = M_{O2} \quad \textbf{(38)}$$

Inerts balance:

$$m_i = M_i \quad \textbf{(39)}$$

where m_{CH4}, m_{H2}, m_{H2O}, m_{CO}, m_{CO2} and m_i are the molar rates of each of the species in the reactor effluent to be determined, M_{H2}, M_C, M_{O2} and M_i are the total moles of each of the elements or inert species in the feed to the reactor.

Next from equilibrium considerations for the reforming reaction,

$$(m^3_{H2} \cdot m_{CO})/(m_{CH4} \cdot m_{H2O} \cdot m^2_{tot}) = Kr \quad \textbf{(40)}$$

and from equilibrium considerations for the water gas shift reaction,

$$(m_{H2} \cdot m_{CO2})/(m_{CO} \cdot m_{H2O}) = Ks \quad \textbf{(41)}$$

where m_{tot} is the total molar rate of the reactor effluent, Kr and Ks are the reaction quotients which correspond to the equilibrium constants for the two reactions at temperatures as specified in order to account for incomplete reactions (i.e., below the actual effluent temperature for the reforming reaction since this reaction is endothermic and above the actual effluent temperature for the shift reaction since this reaction is exothermic).

The six equations above together with the enthalpy balance on the reactor allow the determination of the effluent composition and heat absorption rate.

2.7.2 Reformer Module Results:

The reformer module was tested to determine the predicted performance of a reformer versus several operating conditions and parameters. The parameter variations considered in these analyses included reformer outlet temperature, reformer inlet composition, steam-to-carbon (S/C) ratio, and reformer outlet pressure (Table 4). Please note that Table 4 presents the range of parameters for each of the variations considered. Temperature varied from 427°C to 983°C (800 to 1800°F), S/C varied from 1 to 5, and pressure varied from 15 to 1000 pounds per square inch absolute (psia).

Table 4. Parameter Variations to Demonstrate the Reformer Module

Parameters Changed	Values
Outlet Temperature	800 – 1800°F
Inlet Stream Composition (S/C ratio)	1-5
Inlet Stream Pressure	15-1000 psia

2.7.2.1 Temperature Variations

Figure 12 presents the effect of increasing reformer outlet temperature. The simulation predicts that increasing the reformer outlet temperature increases methane reformation up to the 1250 to 1300°F range. Above this point, the levels remain more or less constant, suggesting that operating above this temperature would not be beneficial as far as reforming the fuel is concerned. A look at the outlet stream higher heating value (HHV) shows a linear decrease that seems to follow the methane concentration level, stopping around 1300°F and remaining constant as the temperature increases. The reformer total energy and heat duty both increase fairly linearly with temperature, leveling off somewhat at high temperatures.

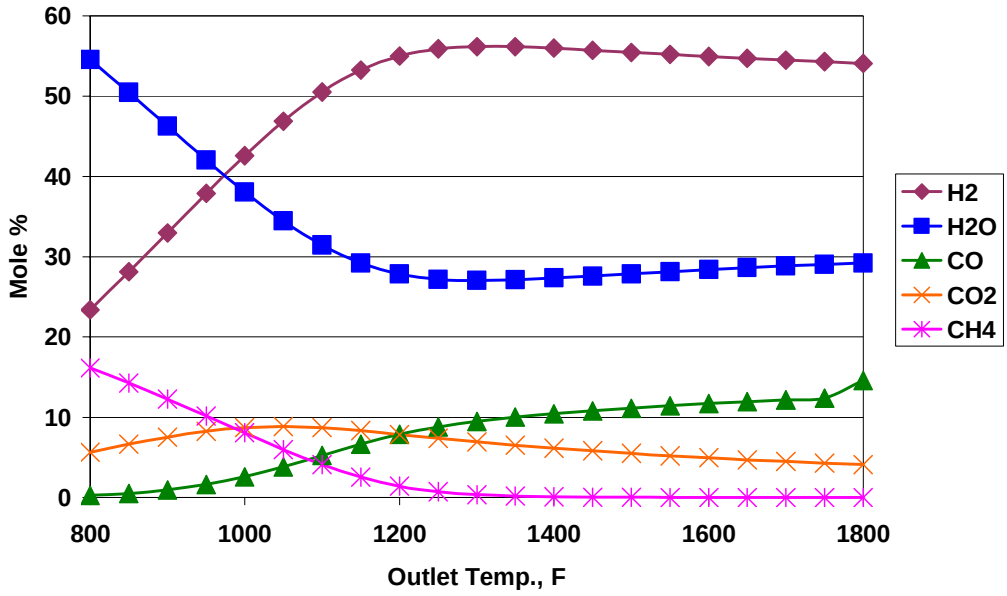

Figure 12. Reformer Temperature on Species Composition at Reformer Exit versus Reformer Exit Temperature

2.7.2.2 Steam-to-Carbon (S/C) Ratio Variations

Figure 13 presents the outlet stream composition versus the steam-to-carbon ratio. The figure shows that the H_2 and H_2O levels nearly mirror one another with increasing S/C ratio (H_2 decreasing and H_2O increasing) until they finally meet around 45 percent at a S/C ratio of 5. Also, the CO level is much lower than H_2, but exhibits a nearly identical response. At the constant temperature given, the CH_4 level is nearly zero for all cases, while the CO_2 level rises slightly. This results in the HHV difference between inlet and outlet reformer streams going to zero at the S/C ratio of 5. The graph of total energy for both reformer streams (inlet and outlet) shows that they both decrease significantly along very similar curves.

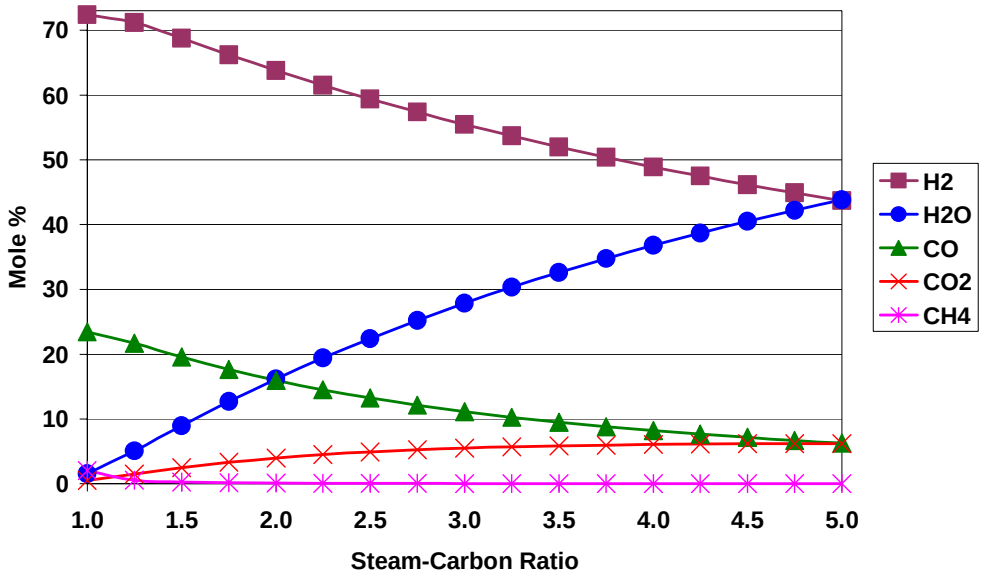

Figure 13. S/C Ratio on Species Composition at Reformer Exit versus Reformer Exit Temperature

2.7.2.3 Pressure Variations

Figure 14 shows the effects of pressure on outlet stream composition. Increases in operating pressure results in reductions in methane reforming. With all other parameters held constant, the increasing pressure causes the H_2 and CO levels to fall, while the CH_4 and H_20 levels rise. This results in a slight increase in the outlet stream HHV, but lower levels of fuel that can be directly oxidized electrochemically within a solid oxide fuel cell (i.e., H_2 and CO). The outlet energy and heat duty of the stream, however, both decrease.

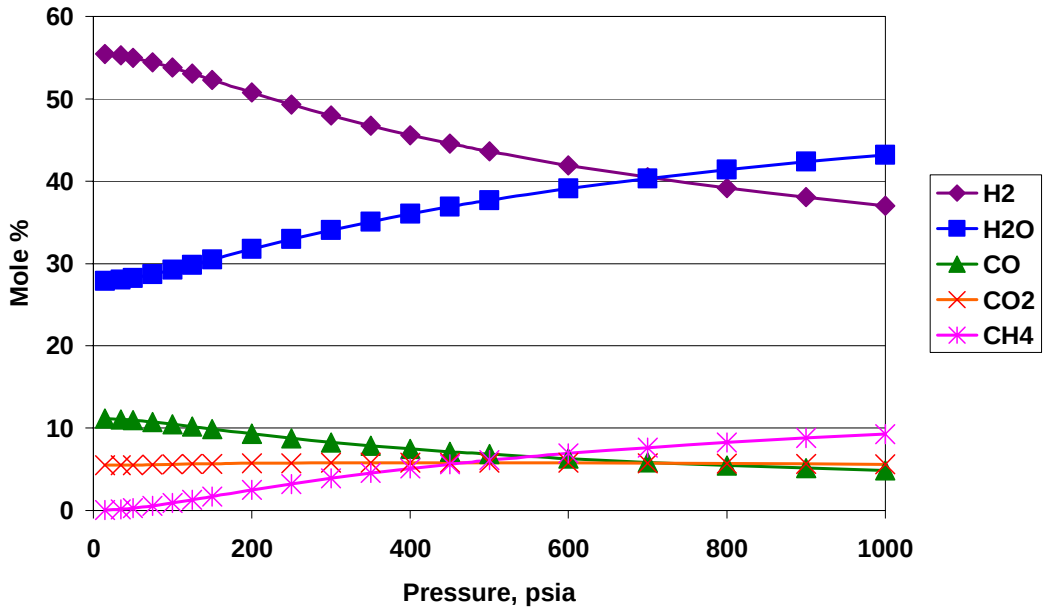

Figure 14. Reformer Pressure on Species Composition at Reformer Exit versus Reformer Exit Temperature

2.8 Gas Turbine Simulation Module

2.8.1 Compressor and Expander Models

The outlet conditions from a compressor and expander (including a steam turbine) are calculated assuming an isentropic path and then applying the appropriate efficiency to determine the actual outlet conditions for a given inlet set of conditions. Thus, for the isentropic compression or expansion:

$$\Delta Si = \Delta So \quad \textbf{(42)}$$

where ΔSi and ΔSo are the inlet and outlet entropies. The adiabatic efficiency, η_A is calculated from the polytropic efficiency, η_P and then used in establishing the actual enthalpy of the stream leaving the unit by:

Compressor:

$$\Delta Ho = \Delta Hi + (\Delta Ho_{,ideal} - \Delta Hi)/\eta_A \quad \textbf{(43)}$$

Expander:

$$\Delta Ho = \Delta Hi + (\Delta Ho_{,ideal} - \Delta Hi)\eta_A \quad \textbf{(44)}$$

where ΔHi and ΔHo are the inlet and outlet enthaplies, $\Delta Ho_{,ideal}$ is the outlet enthalpy corresponding to isentropic path. With the outlet enthalpy established for a given outlet pressure, the temperature is determined. The wok required or produced is given by the difference in the outlet and inlet enthalpies. The efficiency is either user-defined or is calculated by the computer program using empirical relationships.

For the compressor when the inlet flow is greater than or equal to 55 kilograms (kg/s), the following relationship is used as given in the Gas Research Institute Report, (1993)

$$\eta_P = (1.01016 + 8.28/m)^{-1} \quad \textbf{(45)}$$

where m is the corrected mass flow rate at the inlet in kg/s.

When inlet flow is less than 55 kg/s, gas turbine performance data as supplied by General Electric was used to adjust the constants in the previous relationship resulting in the following:

$$\eta_P = (1.2483 + .2239/m)^{-1}, \quad \textbf{(46)}$$

For the gas expander the following relationship is used assuming the same relationship as that for large compressors holds:

$$\eta_P = (1.01016 + 8.28/m)^{-1} \quad \textbf{(47)}$$

For the steam turbine, empirical correlations developed by Spencer et al. (1974) for each of the sections (the high pressure, intermediate pressure and the condensing) are used.

2.8.2 Gas Turbine Model

We developed two types of gas turbine models that may be configured by the user to include multiple compression stages. The first model allows intercooling between the stages and multiple expansion stages with reheat (with combustors) between the stages, and the second models a simple cycle (or conventional Brayton cycle) with no intercooling of the compressor or reheat during expansion.

We configured the user-defined gas turbine model by integrating gas turbine compressor, combustor and gas turbine expander modules. To determine the efficiency of the compressor and expander, we first calibrated a simple cycle engine based on data published by the gas turbine manufacturer, and then applied adjustments to the values determined for the base-line engine. The air required for cooling the blades of the turbine as well as turbine purge air requirements are determined with this same calibration data. The program determines internally the necessary parameters for the base-line engine and for use with the two gas turbine models when the overall gas turbine performance data is specified.

The compressor and expander efficiencies are adjusted for flow through the compressor or expander by utilizing the equations below derived from the equations (45), (46) and (47).

Compressor:

$$\eta_{P1}/\eta_{P2} = (1.1016 + 8.28/m_2)/(1.1016 + 8.28/m_1),\ m_1 \geq 55\ \text{kg/s} \quad \textbf{(48)}$$

$$\eta_{P1}/\eta_{P2} = (1.2483 + 0.2239/m_2)/(1.2483 + 0.2239/m_1),\ m_1 < 55\ \text{kg/s} \quad \textbf{(49)}$$

Expander:

$$\eta_{P1}/\eta_{P2} = (1.1016 + 8.28/m_2)/\ (1.1016 + 8.28/m_1) \quad \textbf{(50)}$$

where the subscripts 1 and 2 refer to the case under consideration and the reference case, respectively.

The turbine-coolant requirement is adjusted in order to maintain the same metal temperature for the first-stage blades of the turbine by utilizing the semi-empirical methodology proposed by El-Masri and Pourkey (1986). This method consists of modeling a combined convective/film cooled blade as a flat plate and developing non-dimensional parameters relating the physical properties of the working fluid and the coolant. The turbine purge requirement is adjusted by maintaining the same velocity as that in the base-line engine. The coolant and purge flows are extracted from upstream of the combustor. Fifty percent of the total coolant used for the first stage stationary vanes or nozzles is considered non-chargeable (does not cost efficiency penalty). It combines with the exhaust from the thermodynamic model of the combustor and the first stage nozzles and flows through the thermodynamic model of the turbine (section of

the turbine downstream of the first stage nozzles) and thus contributes towards producing work in the turbine. The remaining 50 percent of the coolant along with the purge air is considered chargeable and combines with the turbine exhaust and thus performs no work in the turbine (based on data in Gas Research Institute Report, 1993).

The second model assumes that the gas turbine has the same geometry as the gas turbine used for calibrating the engine. The firing temperature and pressure-ratio of the gas turbine are adjusted for variations in flow rate and composition. The pressure-ratio adjustment is made based on the assumption that the Mach number for the flow in the first-stage nozzle of the turbine is at unity (EPRI Report, 1983) by the utilizing following equation:

$$m_1/m_2 = (Mw_1/ Mw_2)^{0.5} (P_1/P_2) (T_2/T_1)^{0.5} \quad \textbf{(51)}$$

where m, Mw, P and T are the mass flow rate, molecular weight, pressure and temperature in the nozzle while the subscripts refer to the case under consideration and the reference case.

The firing temperature is adjusted to maintain the same metal temperature for the first-stage blades as that for the base-line engine since the turbine cooling flows are not controlled.

An empirical correlation is used to adjust the polytropic efficiency of the compressor when the pressure-ratio is higher than the pressure-ratio at design point conditions:

$$\eta_{P1}/\eta_{P2} = (\pi_1/\pi_2)^n \quad \textbf{(52)}$$

where π is the pressure-ratio, n is an empirically determined constant (= 0.4256 derived from performance data for the Nuovo Pignone gas turbine PGT 5B/1 model which has an output of 5.4 megawatt (MW) at International Organization for Standardization (ISO) conditions), and the subscripts refer to the case under consideration and the reference case.

Thus, the model calculates the net gas turbine power output and the exhaust stream for a given air or oxidant entering the compressor and fuel stream entering the combustor while accounting for the cooling requirements of the turbine blades (Figure 15).

The gas turbine model accounts for the changes in the cycle design conditions such as the operating pressure, turbine firing temperature, the fuel and oxidant temperature and composition. The model is calibrated using equipment manufacturer's published performance data in order to use realistic design parameters. Design parameters to reflect projected technological advancements may also be specified.

In this manner consistency is maintained between the different hybrid cycles being investigated (cycles being compared may use streams of different composition, pressure and temperature) since the SOFC and the gas turbine are the two major equipment items in such systems.

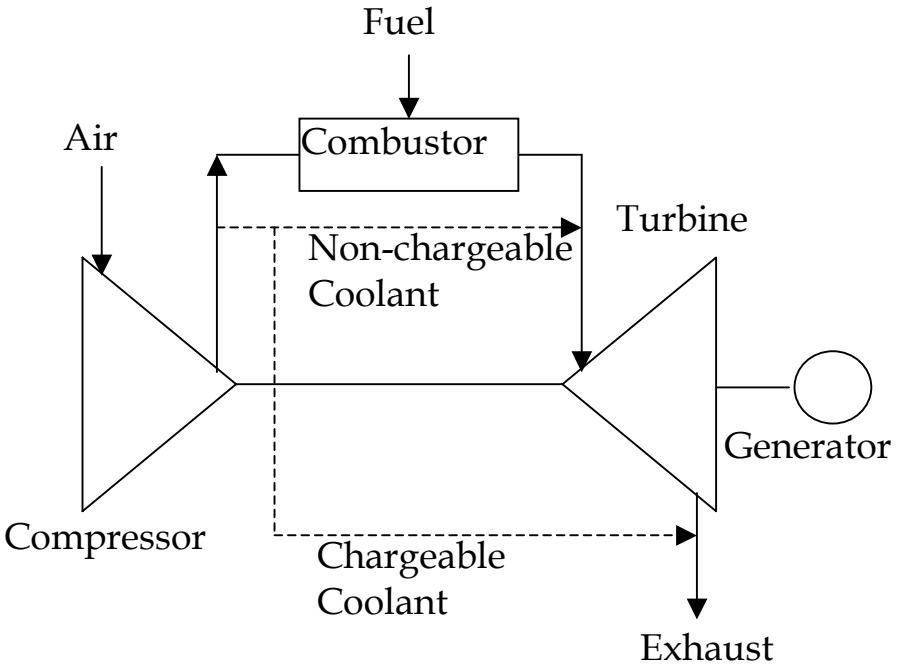

Figure 15. Schematic of Gas Turbine Engine

To accomplish this, a humidifier model was also developed. The humidifier model sizes the column while accounting for the simultaneous heat and mass transfer processes occurring within it and thus provides a basis for selecting cycle conditions that lead to practical column dimensions. An equation of state capable of estimating the enthalpy and entropy corrections for non-ideality of the gas streams is developed in order to handle highly non-ideal streams such as natural gas at pipeline pressures, and supercritical CO_2. A separate property package for steam and water is included.

2.8.3 Gas Turbine Simulation Module

An analysis module for the simulation of a gas turbine engine was developed and tested in the current effort. The module performs a thermodynamic analysis of gas turbine technology, which can be integrated with and used for fuel cell hybrid systems design. Variations in operating parameters, and operating conditions can be accomplished with the module. Included in the analysis module is a DOS-based user interface that allows ready modification of thermodynamic properties, design parameters and conditions of interest. A compiled version of the gas turbine module developed in this period is contained in the diskette provided with this report. The source code for these modules is QuickBasic.

Two types of gas turbine models were developed, one that may be configured by the user to include compressor and expander with variable geometry, and the second consisting of a fixed geometry simple cycle (gas turbine (GASTURB) module). First step consists of calibrating a simple cycle engine based on data published by the gas turbine manufacturer, and then applying adjustments to the values determined for the "base-line engine." The program

determines internally the necessary parameters for the base-line engine and for use with the two gas turbine models when the overall gas turbine performance data is specified.

Representative results from the Gas Turbine Module are presented in the following figures. Note that all of these calculations are made for simple cycle gas turbine engines. All of the simulations were performed by first calibrating the model to a single data point available for each of the simple cycle gas turbine engines simulated. Table 5 provides the calibration data used for the 1-megawatt (MW) simple cycle system while Figure 16.presents the results from the simulation. Note that the 1 MW turbine predictions show a minimum efficiency point at about 70 percent load with higher efficiencies for either higher or lower output. This is quite unusual and is attributed to the small size of the unit.

Table 5. Gas Turbine Calibration Data (1 MW System)

1 MW Rated Simple Cycle Gas Turbine	
Model	**PW – STGL-90**
Net Output, kW	1175
UHV Heat Rate, Btu/kWh	12212
Pressure ratio	10.4
Air flow, lb/s	11.6
Turbine inlet temperature, degrees F	1800
Exhaust temperature, degrees F	997
Air Stream Data	
Rate, lb/s	11.6
Temperature, F	60
Pressure, psia	15
Fuel Stream Data	
Rate, lb/s	1.1
Temperature, F	100
Pressure, psia	250
Turbine Data	
Exhaust pressure, psia	15

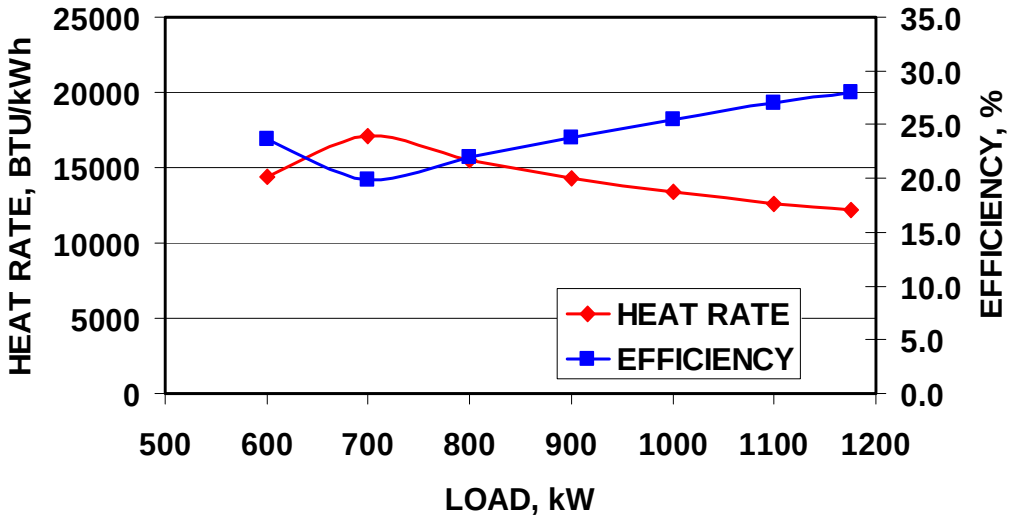

Figure 16. Calculated Heat Rate and Efficiency versus Load (1 MW System)

The simulation results presented in Figure 17 are for a 50 MW simple cycle gas turbine engine. The calibration data (Table 6) used for this case indicate a heat rate of 10,450 British thermal unit (BTU)/kilowatt hour (kWh) at full load (49.5 MW). In this case the model results indicate monotonically decreasing efficiencies (increasing heat rates) with decreases in load (Figure 17). This is typical of simple cycle gas turbine engines, which are usually less efficient at part load conditions.

Table 6. Gas Turbine Calibration Data (50 MW System)

50 MW Rated Simple Cycle Gas Turbine	
Model	**SW – W251B11/12**
Net Output, kW	49500
UHV Heat Rate, Btu/kWh	10450
Pressure ratio	15.3
Air flow, lb/s	386
Turbine inlet temperature, degrees F	2150
Exhaust temperature, degrees F	957
Air Stream Data	
Rate, lb/s	386
Temperature, F	60
Pressure, psia	15
Fuel Stream Data	
Rate, lb/s	11.5
Temperature, F	100
Pressure, psia	350
Turbine Data	
Exhaust pressure, psia	15

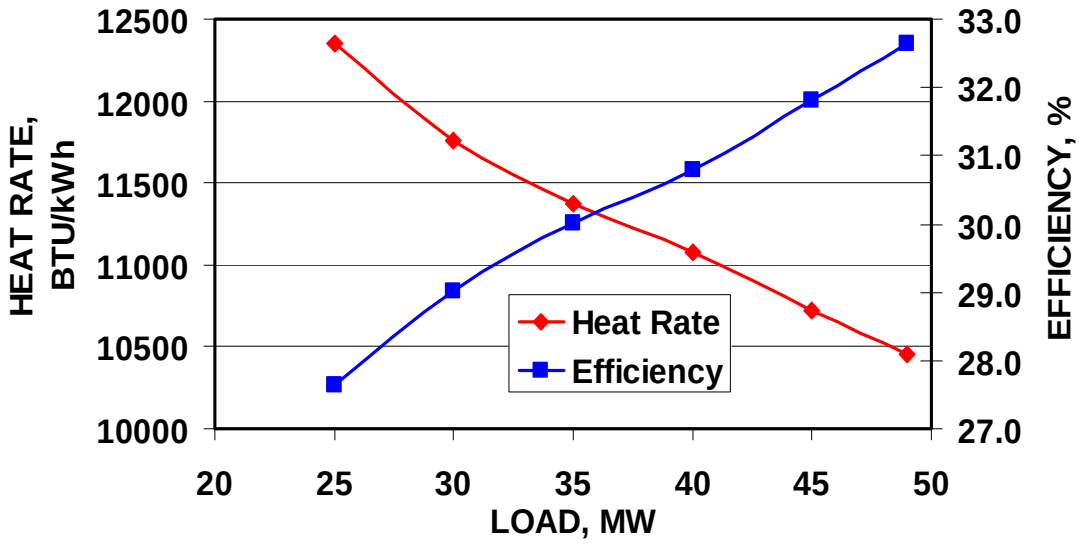

Figure 17. Calculated Heat Rate and Efficiency versus Load (50 MW System)

Figure 18 presents results from the 190 MW simple cycle gas turbine engine simulations. The calibration data (Table 7) used indicate a heat rate of 9670 BTU/kWh at full load (189 MW). In this case the model results indicate monotonically decreasing efficiencies (increasing heat rates) with decreases in load (Figure 18). This is typical of simple cycle gas turbine engines, which are usually less efficient at part load conditions.

Table 7. Gas Turbine Calibration Data (190 MW System)

190 MW Rated Simple Cycle Gas Turbine	
Model	**SW – V94.2**
Net Output, kW	189000
UHV Heat Rate, Btu/kWh	9670
Pressure ratio	14
Air flow, lb/s	1147
Turbine inlet temperature, degrees F	2150
Exhaust temperature, degrees F	1085
Air Stream Data	
Rate, lb/s	1147
Temperature, F	60
Pressure, psia	15
Fuel Stream Data	
Rate, lb/s	20.3
Temperature, F	100
Pressure, psia	350
Turbine Data	
Exhaust pressure, psia	15

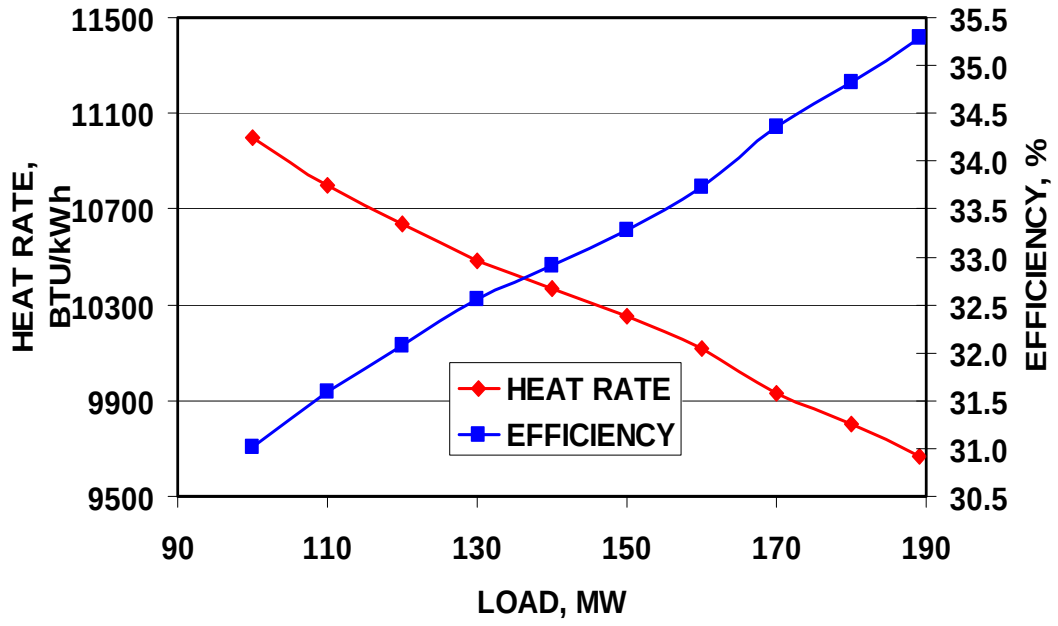

Figure 18. Calculated Heat Rate and Efficiency versus Load (190 MW System)

2.9 Standardized Analysis Format

In order to compare various system configurations on a consistent basis, a design criteria is established as summarized in Table 8. Additional criteria will be established as the cycle analysis part of this research program proceeds.

The Siemens Westinghouse Power Corporation SureCell™ configuration, as depicted in Figure 19, is selected as the Base Cycle over which improvements made by new configurations are quantified.

An Exergy analysis is performed for each of the system configurations in order to explain quantitatively the difference in the overall efficiency of the configuration over the Base Cycle. Exergy analysis is also beneficial in order to identify the major sources of inefficiency in the system so that improvements may be directed towards these specific areas of the system.

Table 8. Design Criteria for Standardized Analysis Format

Design Parameter	Value
Ambient Dry Bulb Temperature	15 °C[1]
Ambient Relative Humidity	60%[1]
Elevation	sea level[1]
Fuel	Natural gas
Fuel Supply Pressure	20 bar A
SOFC Operating Pressure	15 barA maximum
Gas Turbine Firing Temperature	1200°C maximum
Gas Turbine Exhaust Pressure Drop	.033 bar
Gas Turbine Exhaust Heat Loss	0.5%
Steam Generator Pinch Temperature	9°C minimum
Boiler Feed Water Sub-cooling to Evaporator	9°C minimum
Steam Drum or Humidifier Blowdown	0.5% of evaporation rate
Shift Reaction Approach to Equilibrium	15°C
Reforming Reaction Approach to Equilibrium	25°C
Pressure Drop in Heat Exchangers	2% minimum
Temperature Approach in Heat Exchangers	10°C minimum

[1] International Organization for Standardization (ISO) conditions

2.9.1 Applications Strategy

Hybrid systems are configured such that (1) the overall system efficiency is maximized and (2) simplicity is maintained in order to not compromise plant capital cost and process controllability. System performance is developed for various operating pressures of the SOFC, the gas turbine and the steam cycle when included in the system under investigation while staying within the constraints of the Design Criteria in order to develop the optimum system performance.

The above represents a standardized format for industry to evaluate their own methods and to provide an anchor for comparison between the various technology providers' results. In addition, since the Siemens-Westinghouse SureCell™ design will be the first hybrid system that is experimentally tested, the analysis format and strategy can be validated in the future to firmly establish the basis of the Standardized Analysis Format described above.

The Standardized Analysis format presented herein will be enhanced and finalized in the out-years of the current effort. Review, comments, suggestions and necessary modifications to the analysis strategy are solicited from the California Energy Commission and will be solicited from the Industrial Advisory Team that is to be established in these out-years of the current effort.

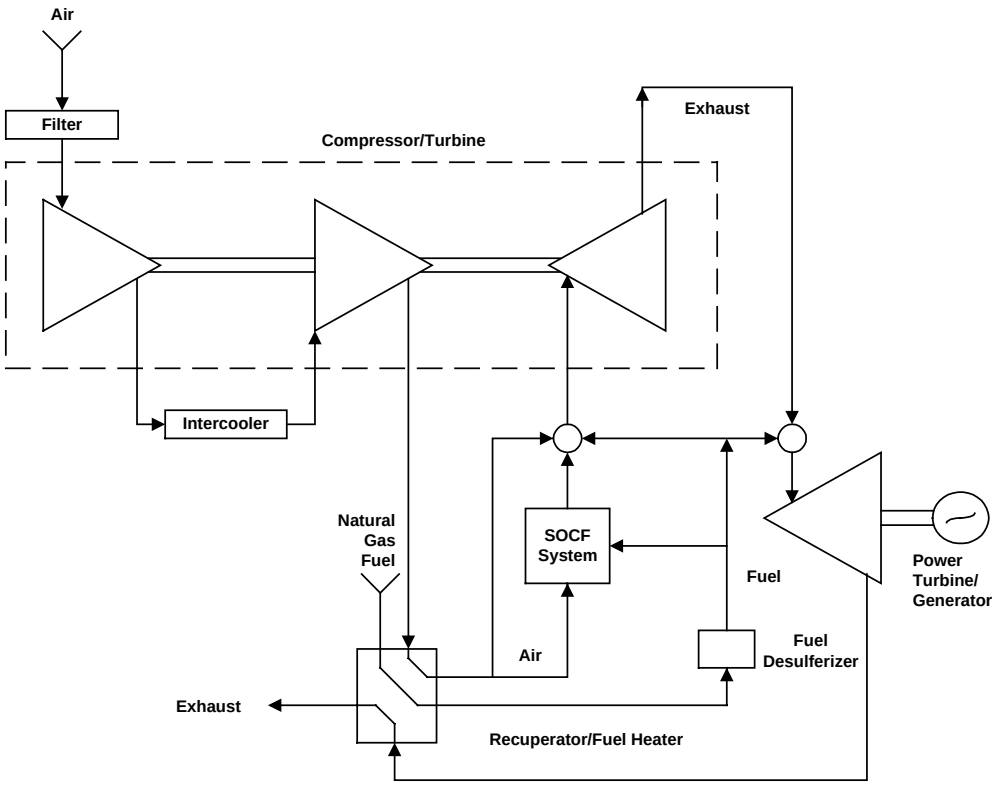

Figure 19. The Siemens Westinghouse Power Corporation SureCell™ configuration

2.10 Energy Tutorial

An energy tutorial was developed for this program for application on the World Wide Web. The concept was to develop educational resources regarding energy and fuel cells that would allow instruction via the Internet to a broad community interested in the energy field. The entire text of the tutorial was delivered to the Commission under cover of the second quarterly progress report. The outline of the Internet tutorial is as follows:

1. Energy
2. GNP
3. Fossil Fuels
    3.1. Natural Gas
    3.2. Petroleum/Oil
    3.3. Coal
4. Oil Shale
5. Nuclear
6. Solar
7. Wind
8. Geothermal
9. Biomass and Wastes
10. Hydroelectric
11. Energy Conversion
12. Fuel Cell
    12.1. PAFC
    12.2. Molten Carbonate Fuel Cell (MCFC)
    12.3. SOFC
    12.4. PEMFC
13. Combustion
14. Gasification
15. Environmental Impacts
16. Trends
17. Reciprocating Engine
18. Gas Turbine
19. Steam Turbine

The energy tutorial outlined above contains photos, graphics, charts and questionnaires that convey energy instruction via the Internet. The HTML document prepared for this effort is currently posted on the Internet under the NFCRC web-site. The URL for this site is:

http://www.nfcrc.uci.edu/tutorial/tableofcontents.html

Some key features of the tutorial include:

- Font and text formatting for readability and ease of use,
- Pictures and graphics illustrating various energy concepts,
- Questionnaires for interactive learning,
- Links within and amongst the various aspects and parts of the tutorial,
- Search engine,
- Discussion page,
- Title bar for navigation, and
- Links to other organizations providing useful and objective information (per suggestion of the Energy Commission project manager).

3.0 Task 2: Technology Transfer

Technology Transfer for Fuel Cells and Fuel Cell Systems has been accomplished in the current program in three separate areas (1) Multi-Functional Room (MF), (2) Educational Facility for Ambient Air Monitoring (EFAAM), and (3) NFCRC Web-Site. The first technology transfer element (MF) included the design, purchase and installation of display and projection equipment, switching equipment, an integrated control system, technology transfer accommodations, and miscellaneous integration and control components. This task was accomplished in collaboration with the Intellisys Group. The second area of technology transfer accomplishments included designing and installing an interactive educational facility for instruction and insight into both global climate change and urban air pollution issues. The third area of technology transfer accomplishments included a major design and implementation effort focused on the NFCRC web site. The accomplishments in each of these areas are presented in more detail below.

3.1 Multi-Functional Room

Design and installation of technology transfer infrastructure was accomplished in the current contract. This installation was completed in the Multi-Functional (MF) room of NFCRC. We hired an audio/visual (A/V) consultant to design an integrated A/V package for technology transfer. The Intellisys Group was hired to fully design an integrated A/V system for the Multi-Functional room of the NFCRC. The design for technology transfer included:

- Computer Internet and local area network access
- Teleconferencing design
- Multi-channel microphone system
- Video-conferencing design
- Integrated touch controls
- Audio Visual Presentation system design for
  - Overhead projection
  - Slide projection
  - Digital VGA projection
  - Television signal projection
- Integrated design for central control of lighting, shades and above systems

The major elements of the MF room infrastructure that were designed, installed and used in the current effort are:

- An audiovisual system,
- A display and projection system,
- An integrated control system,

- Miscellaneous integration and control equipment, and
- Technology transfer accommodations.

Each of these elements is described in more detail below.

3.1.1 Purpose of the MF Room Design and Installation

This project designed, installed, and used a technology transfer infrastructure in the MF room of the NFCRC as part of the current technology transfer effort. The goal of the overall system is to provide a flexible technology transfer environment that supports five primary technology transfer scenarios:

- **1-5 day Short Courses**. Classroom style seating with seating for up to 48 people with electrical and Internet access, audio and video conferencing capabilities, and clear views of projected and written information on fuel cells and hybrid systems.
- **Technology Society Meetings**. U-shaped table set up and potential for classroom style seating for up to 48 participants with electrical and Internet access, audio and video conferencing capabilities, and clear views of projected and written information on fuel cells and hybrid systems.
- **Half-Day Workshops and Meetings**. Various table and A/V system configurations to accommodate the variety of fuel cell and energy instruction required to facilitate education and adoption of fuel cell and fuel cell hybrid systems in California.
- **Advisory Council Meetings**. Round or Square Table configuration to accommodate 20-25 people all with microphones and speaker stations on the table to advise, provide counsel and insight to the NFCRC.
- **Fuel Cell Stakeholder Meetings**. Various table and A/V system configurations to accommodate the variety of fuel cell and energy technology transfer required for visits of fuel cell and related companies, regulators, politicians, agency representatives, and energy decision-makers.

During the current effort, the MF room was used for local presentations, workshops, classroom instruction, and several audio and videoconferences.

3.1.2 Funding Support

Funding to support the design and installation of the majority of the A/V components of the MF room technology transfer system was provided by the current Public Interest Energy Research (PIER) contract with the California Energy Commission. Some aspects of the audiovisual system, however, were supported by a separate grant administered by the California Energy Commission entitled “Technology Transfer for Fuel Cell Systems,” which is supported by the Petroleum Violation Escrow Account (PVEA) program as grant number MEM-97K-031. The current PIER contract supported the complete design and the purchase and installation of the following aspects of this MF room technology transfer system:

- Display and Projection Equipment
- Switching Equipment
- Integrated Technology Transfer Control System

- Technology Transfer Accommodations
- Miscellaneous Integration and Control Components

For the record, the PVEA grant supported the purchase and installation of the following aspects of the MF room technology transfer system:

- Integrated Video-Conferencing System
- Computer Floor Installed Data Network System
- Technology Transfer Audio System

The following MF room technology transfer components, which were fully supported by the current PIER contract, are described in more detail in the following sections.

3.1.3 Technology Transfer Display and Projection System

The projection system has been fully designed and consists of a ceiling-mounted LCD video/data projector, on a fixed enclosure, capable of displaying standard National Television System Committee (NTSC) video signals, and computer source signals up to SXGA resolution on a front projection surface. The location of the projector at the rear of the room requires the use of a long throw zoom lens.

A 35mm projector with a long throw lens is located in the same enclosure. The slide projector is installed on a slide out shelf allowing the slide carousel to be changed. The enclosure also houses an auxiliary camera for the video conferencing system.

The video system includes the capability to display VHS tapes from a single 4-head videocassette player/recorder, a high-resolution document camera, a digital video disc (DVD) player, five computer sources, and auxiliary video sources connected to the system as required. Computer interfaces (TTL/Analog) are located in the cabinetry housing the dedicated computer, the podium, and floor boxes are used to connect computers to the system. Connections for keyboard and mouse control of the dedicated computer are available at the podium, and at three of the floor boxes, with the use of a keyboard mouse switching system.

A video conferencing system is interconnected to the large screen display that is described later in this document. Additionally, three cameras are remotely located in three of the labs on the NFCRC.

3.1.4 Switching Equipment

The switching equipment provides the ability to route information to any of the audio-video equipment (i.e. podium, or videoconference monitor) within the training center. This ability provides a great deal of flexibility for the transferring and displaying of information within the technology transfer training center.

3.1.5 Integrated Technology Transfer Control System

An integrated remote control system is included in the system that was installed in the Multi-Functional room. This capability allows users the ability to operate system components using icon-based LCD touch-screens. Two (2) color touch panels are a part of the system. One touch

screen is hard wired and installed in the podium while the other can be connected at four separate floor box locations.

The system integrates the most commonly used needs of the presenter or operator. Included are: Play, Stop, Fast Forward, and Reverse on the VCR, DVD, cassette recorder; channel Up and Down on the TV tuner, source selection, volume Up and Down, projection screen Up and Down, and projector On and Off, video conferencing controls, audio conferencing controls. If the lighting system is reworked to include an electronic dimming system, the control system can also control the lights from the panel to bring up pre set lighting options. The panel also provides the dialing interface for the audio teleconferencing system.

A 16 button wireless remote is a part of the system allowing control of the 35mm slide projector ON, OFF, FWD, REV, FOCUS IN, FOCUS OUT. Other functions may also be requested by NFCRC such as lighting or VCR control form this wireless panel, up to 16 buttons.

3.1.6 Technology Transfer Accommodations

The accommodations required for effective technology transfer in the Training Center (NFCRC MF room) include furniture that provides participants in technology transfer activities with access to the internet, access to electrical power, classroom features such as write boards, tables, and flexible seating to accommodate multiple configurations. The current effort supported the design and installation of these technology transfer accommodations.

In addition to these accommodations, a ceiling-mounted enclosure houses a projection system that includes the LCD video/data projector, 35 mm slide projector, and an auxiliary camera for the video conferencing system. The enclosure is of steel construction, with a powder-coated white finish, and has a hinged front door with a glass opening and a louvered top with a vent fan. The bottom third of the rear panel contains a louver allowing air intake. The enclosure is lined with acoustic absorption material, and contains a ceiling attachment pole with cable access from the top of the unit. The enclosure can be raised and lowered automatically using the integrated control system.

3.1.7 Miscellaneous Integration and Control Components

The two primary miscellaneous components included in the current effort are a podium and an electronic white board. The podium houses the items mentioned in the Integrated Technology Transfer Control System section. From this single location most of the features of the MF room technology transfer system components can be controlled.

The electronic white board is wall mounted and connected to the host computer via a serial connection for display on the large screen, capture for recording and printing to one of the network printers. The board allows notes to be saved in four-color electronic files.

3.1.8 Equipment Description and Photographs

Figure 20 shows the inside of the ceiling mounted enclosure for display equipment. Three of the display and projection devices used in the MF room technology transfer system are shown. The enclosure and equipment are located in the rear of the MF Room. The cabinet is raised and lowered via a motorized lift. The cabinet contains a LCD projector (top shelf), a 35mm slide projector (middle shelf), and a remote camera (bottom shelf).

An equipment rack that contains much of the audio visual and control equipment was installed in a corner cabinet in the front left-hand side of the MF room. Contained within the equipment rack are several projection and display equipment components as well as switching and routing components. The equipment rack houses the two VHS cassette decks, an audio recording system, a CD player, a DVD player, and audio and video switchgear. These components can record, play, and route audio and video sources to and from the various audio/video system components.

Figure 20. Display and Projection Equipment

Figure 21 shows the touch screen for the technology transfer control system. From this screen all the features of the A/V system can be accessed, monitored, and controlled. This feature makes the entire system very user friendly.

Figure 21. Integrated Technology Transfer Control System

Figure 22 shows the tables and chairs of the Technology Transfer Accommodations. The tables and chairs may be configured in many ways to accommodate the various types of activities that will be hosted within the multi-function room. Also shown are the podium and electronic white board that are few of the miscellaneous components. The electronic smart-board is located to the left of the large corner cabinet containing the equipment rack. The subtle integration of these important components makes the room aesthetically pleasing as well as functional.

Figure 22. Technology Transfer Accommodations

3.2 Educational Facility For Ambient Air Monitoring

To further facilitate the NFCRC goals of research, education, and technology transfer, we have conceptualized, developed, designed and installed a device designated the Educational Facility for Ambient Air Monitoring (EFAAM). The purpose of this facility is to provide technology transfer and education for NFCRC visitors via interactive access to data and trends representing global climate change and urban air pollution. Public awareness regarding these environmental concerns is instrumental to the focus and goal of promoting clean, environmentally preferred fuel cell power technology to the general public.

Figure 23 shows completed EFAAM installation in the NFCRC gallery. In its physical appearance, the EFAAM consists of a Horiba air quality-monitoring console and two interactive computer monitors for analysis and presentation of information. The Horiba console is visible in the upper right-hand corner. It stands about six feet tall and is approximately twenty inches wide.

Figure 23. The EFAAM Installation

3.2.1 Educational Features

The EFAAM serves as the main interactive point-of-information in the NFCRC Gallery. Visitors can toggle between several active and interactive displays to examine real-time ambient and indoor air quality monitoring; view slide shows pertaining to pollutant gas species, global climate change and the human impact on the atmosphere; and surf the Internet for sites pertinent to meteorology, pollution, and global warming.

Visitors can view two educational slide show presentations (Appendix II). The Global Climate Change presentation discusses the impacts of greenhouse gasses and global warming. Using objective data from numerous sources, this presentation examines the major sources of greenhouse gasses including transportation, industry, and power production. The presentation looks at California's role in reducing greenhouse emissions and compares the state's progress with that of the nation and the world. The impacts of the consumption of fossil fuels are studied and linked to increases in environmental CO_2 over time. The presentation also includes an emphasis on the sources and control of methane gas. Finally, the key resolutions of the Kyoto Protocol and its anticipated impact to reverse global warming are summarized.

The Urban Air Pollution slide show focuses on nitrogen oxide ($NO_{x)}$, CO, ozone ($O_{3)}$, and particulate matter, explaining how each reduces the healthfulness of the ambient air. The presentation provides an explanation of California's approach to pollutant monitoring via air basins. It looks into the production of the culprit species and chronicles pollutant levels on a state and national basis. The slide show examines emission trends and shows how tight air quality legislation in California is reducing air pollution. Specific information including a listing of the most polluted cities in the USA as well as state and federal attainment and non-attainment designations for each species are also provided.

3.2.2 Gas Analyzers

The facility has the capability to accurately measure atmospheric concentrations of ozone, oxides of nitrogen (NO, NO_2, NO_x), carbon monoxide, hydrocarbons (CH_4, non-methane hydrocarbons), and carbon dioxide.

Nitrogen Oxides Measurement

A HORIBA APNA-360 gas monitor employing the method of chemiluminescence continuously measures oxides of nitrogen in sampled air. Ozone is generated in an onboard generator and reacted with sample air. Any NO in the atmospheric sample gas is reacted with the O_3 creating products as well as dispersion of light in the 600—3000nm range. This light output is proportional to the concentration of NO present. The machine is also capable of measuring NO_X (the sum of NO and NO_2) by running the air sample through a "NO_X converter" that converts all NO_2 into NO. The air sample is then reacted and the concentration of total NO_X is obtained.

Ozone Measurement

Ozone is continuously measured using a Horiba APOA-360 analyzer. An ultraviolet absorption method is used to determine the O_3 concentration on the air sample. An internal lamp emits ultraviolet light at a wavelength of 2537 Angstroms over which the air sample flows. A detector, looking through the sample gas at the light source, records the remaining light energy not absorbed by the gas; the amount of light absorbed is proportional to the concentration.

Hydrocarbon Measurement

A Horiba APHA-360 analyzer is used to continuously measure ambient levels of hydrocarbons using flame ionization detection (FID) combined with selective-combustion. The air sample is passed through a hydrogen flame surrounded by a high-voltage differential sensor. Hydrocarbons in the air cause the energy of combustion to increase and therefore increase the current potential surrounding the flame in a fashion proportional to the concentration of

hydrocarbons. By employing selective-combustion, the concentrations of methane and non-methane hydrocarbons can each be determined.

Carbon Monoxide Measurement

A Horiba APMA-360 analyzer continuously measures carbon monoxide concentrations in the sampled air. The non-dispersive infrared technique is employed to measure the CO concentration in the atmospheric sample. Sample gas and a reference gas are alternately injected into a cell. Infrared light is passed through the cell and residual energy is detected. The change in residual energy indicates the concentration of CO relative to the reference gas concentration.

Carbon Dioxide Measurement

A Horiba VIA-510 analyzer continuously measures carbon dioxide concentrations in the sampled air. It also uses the NDIR method in a manner much like the carbon monoxide monitor.

3.2.3 Gas Farm

The EFAAM system is calibrated every evening from baseline gasses stored outside of the NFCRC in a protected breezeway. Six pressurized cylinders containing known concentrations of NO/NO_2, CO, CO_2, hydrocarbons, hydrogen, and zero air supply the EFAAM with calibration gas for mixing. The gasses travel about 100 feet through Teflon tubing housed in conduit to reach the indoor air monitors. Figure 24 shows the gas inputs.

Figure 24. Span Gas Injection Manifold

3.2.4 Gas Calibration Unit

An Environics gas calibration unit precisely blends the supplied reference gas and air with or without ozone. Ozone is generated within the instrument from the supplied bottled zero air. Each calibration gas is blended using a mixing chamber and thermal mass flow meters to insure an accurate mélange at a continuous flow rate.

The Environics unit accurately monitors calibration and intermittent spike checking. Periodically, each analyzer is automatically spiked with three known gas concentrations within each monitor's respective range to ensure both calibration and linearity of reported data. These

data are logged and any deviation between the known and measured concentrations (outside of experimental error and monitor accuracy) is used to inform the NFCRC of system service and repair requirements. This calibration procedure operates in accordance to California's South Coast Air Quality Management District (SCAQMD) standards and specifications for an ambient air monitoring station.

3.2.5 Meteorology Measurements

On the roof of the NFCRC, a facility exists to measure the ambient weather conditions. The installation consists of a rain gauge, pyranometer, thermometer, relative humidity sensor, and barometer (Figure 25).

Figure 25. EFAAM Meteorological Equipment Station Installed Atop the Engineering Laboratory Facility

Two hundred yards away, on top of UC Irvine's 10-story Engineering Tower, an anemometer with integrated wind vane is installed atop a 25-foot tower. (Figure 26) shows a close-up image of the anemometer. From the Engineering Tower, the wind-speed and direction data are transmitted to the NFCRC via infrared transmitter/receiver system.

Figure 26. Wind Anemometer Installed Atop the Engineering Tower

3.2.6 Computer System

Each instrument mentioned in the proceeding sections transmits analog signals (0—1 volt (V), 4—40 milliampere (mA)) proportional to each respective value measured. The signals are interpreted using a National Instruments Fieldpoint Analog Input Module, capable of up to 16 channels of analog input at one hertz (Hz) sampling frequency. The Fieldpoint is connected to the serial port of a personal computer and read using a National Instruments Labview data acquisition and interpretation program. Labview is a graphical programming language designed specifically for data acquisition.

The Labview program reads the instrument input and converts the raw data into visual displays indicating weather and air quality running on a continuous loop on one of the EFAAM's monitors. Figure 27 and Figure 28 show two sample display screens. All data are recorded once each hour by the Labview program and saved in database format for future analysis.

The indoor measurements are most interesting to visitors of the NFCRC in that they can easily take note of the significant rise in CO_2 and other due to the human habitation and respiration in the NFCRC.

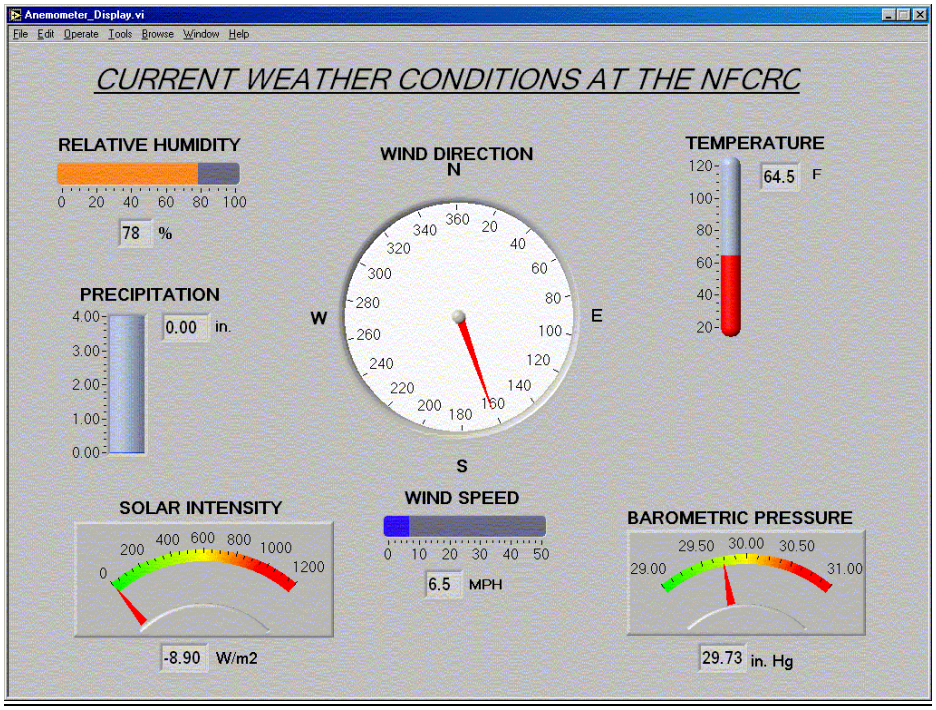

Figure 27. Meteorology Display Screen

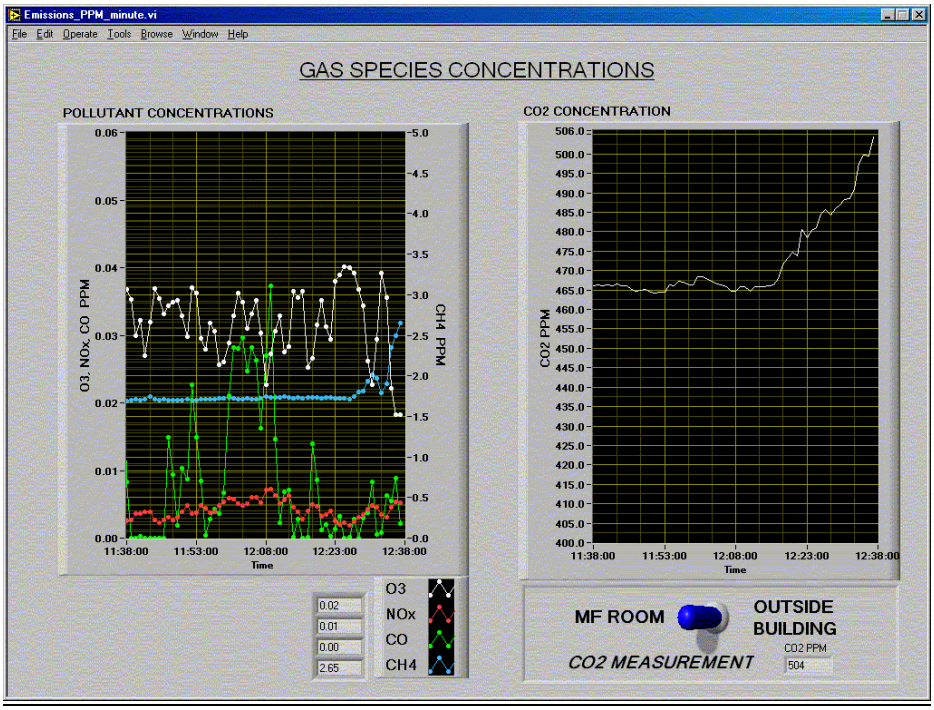

Figure 28. Air Quality One Minute Average Slide

3.2.7 Installation

Ambient air is sampled from two locations: outside the NFCRC and within the Multi-Functional Room. Air samples travel through stainless steel or Teflon lines to avoid contamination and are sucked into the analyzer stand via a supplemental Teflon diaphragm pump to overcome frictional losses associated with the long sample lines. The pump outlet is connected to a stainless steel plenum from which each analyzer takes its air sample. Excess sample gas and analyzer exhausts are vented through a common port to the outside.

In order for the gas analyzers to be calibrated, the Environics gas mixer is plumbed to each analyzer's calibration inlet to deliver a known concentration of calibration gas. This same line is also plumbed to the supplemental pump's inlet to allow for "spiking" the analyzers.

SCAQMD Specifications

It is the ultimate intention that the EFAAM serve as the ambient air monitoring station for the Irvine area within the SCAQMD data network. For that reason, the calibration, sample collection, and sample analysis procedures are compliant with the SCAQMD's air quality monitoring standards.

3.3 National Fuel Cell Research Center & Advanced Power and Energy Program Web Sites

The design of the NFCRC web site has been completed. Table 9 provides an outline of the site with appropriate URLs listed for direct access to the current site via MS Word.

Table 9. National Fuel Cell Research Center Web Site

About NFCRC
Projects
Concept
Focusing Alliancing Center
Bridge Concept
Alliances
Press Release
Personnel
Virtual Tour
Contact
Fuel Cell Information
What is a Fuel Cell?
Manufacturers
Users
Research Development
Technical Database
Information & Contents
General Information
Education
Technology Advancement
Virtual Lab
Outreach
Member Services
Guest Access
Information Request
NFCRC Members
Founders
Affiliates & Members
Services
Benefits
Registration
Educational Resources
edu/edu.htmedu/edu.htm
Related Web-Sites
links/links.htmlinks/links.htm
What's New
Contacts

Several aspects of the NFCRC web site were updated to contain the latest information for technology transfer. These areas include the related web-sites area as well as the Manufacturers Users and Developers of fuel cells sections. In addition, the University of California Irvine (UCI)

campus approved in this quarter the title of Advanced Power and Energy Program (APEP) to define the overall program directed by Professor Scott Samuelsen in fuel cells, gas turbines, power generation and the environment. An overview web site contained at:

http://www.apep.uci.edu

This site describes the activities accomplished at the NFCRC and enhances the technology transfer for fuel cells and fuel cell systems by placing them in the context of the evolving advanced power and energy technologies and market. Described under the APEP site are the NFCRC, UCI Combustion Laboratory (UCICL), Distributed Technologies Testing Facility (DTTF), Living Laboratory (L2), and the Pacific Rim Consortium on Energy Combustion and the Environment (PARCON).

4.0 Outcomes

- The initial development of steady state analyses tools for fuel cell systems and cycles was completed with the development and demonstration of simulation modules for:
  - tubular SOFC
  - steam reformer
  - gas turbine engine
- Technology transfer infrastructure for effective communication and information dissemination about fuel cells and fuel cell hybrid systems was accomplished in three separate areas:
  - Multi-Functional Room
  - EFAAM
  - NFCRC Web Site

4.1 SOFC Simulation Module

An analysis module for the simulation of tubular solid oxide fuel cells (SOFC) was developed and tested. The module performs a thermodynamic analysis of the performance of tubular SOFC technology for a variety of fuel cell stack and systems designs, operating parameters, fuel and oxidant properties, and operating conditions. Included in the analysis module is a DOS-based user interface that allows ready modification of thermodynamic properties, design parameters and conditions of interest.

4.1.1 Steady State Analyses Tools Development

The initial development of steady state analyses tools for fuel cell systems and cycles has been completed with the development and demonstration of simulation modules for: (1) a tubular solid oxide fuel cell (SOFC), (2) a steam reformer, and (3) a gas turbine engine. These modules will serve as the basis for the overall steady state analyses tools that are being developed for complete fuel cell and fuel cell hybrid systems.

The SOFC module simulates a tubular design based upon the fundamental mechanisms that govern fuel cell operation. The model is superior to other models reported in the literature and contains a rigorous treatment of the major heat transfer mechanisms (conduction, convection, radiation), and accurate accounting of pore diffusion & adsorption of oxygen for cathode mass transfer. In addition, the SOFC module contains accurate accounting of all cell irreversibilities (activation, concentration, and ohmic polarization), and precise considerations for fuel stream properties allowing use of H_2, CO, CH_4 as fuels and including shift reaction equilibrium chemistry. Unlike the models in the literature, which are based on finite element approaches, the current model uses an integral approach.

The SOFC module results, without arbitrary parameter variations to match data, well matched available data for the performance of Siemens Westinghouse Power Corporation technology versus pressure and current density. Although the model does not perfectly match the data, the logarithmic dependence upon pressure and the general trends versus current density are well matched providing confidence in the performance of the SOFC module.

The reformer module was able to demonstrate the effects of operating pressure, operating temperature and steam-to-carbon (S/C) ratio on the production of hydrogen and carbon monoxide from natural gas (methane). Reformation chemistry and reformer performance (increased conversion of CH_4 to H_2 and CO) was enhanced with increases in operating temperature up to about 1300^{o}F. Decreased production of H_2 and CO was observed with increases in S/C ratio and pressure.

The gas turbine engine module was able to simulate the performance of several different gas turbine engines including: (1) a 1 MW, Pratt and Whitney simple cycle machine, (2) a 50 MW Siemens Westinghouse simple cycle machine, and (3) a 190 MW Siemens Westinghouse simple cycle machine. These simulations were accomplished by calibrating the model versus available data for steady state performance at full-load conditions. In each case the efficiency of these gas turbine engines was reduced (heat rate was increased) under part-load conditions. The 190 MW system exhibited efficiencies between 31 percent and 35 percent on a lower heating value (LHV) basis. The 50 MW and 1 MW systems exhibited efficiency ranges of 27.5 – 32.5 percent and 20 – 27 percent, respectively, on the same LHV basis.

4.1.2 Technology Transfer for Fuel Cells

Technology transfer for fuel cell systems and cycles was accomplished by the NFCRC, serving as an objective source for information on the state-of-the-art for fuel cells and other advanced power generation technologies. The NFCRC continues to present fuel cell systems and cycles as well as the manufacturers and developers of such systems in a neutral and objective fashion accounting for the reliability and other performance characteristics of each technology as well as the life cycle impacts of each technology. Comparisons amongst technology types and amongst specific developers and manufacturer's products can be made since the NFCRC works with most of the stationary fuel cell manufacturers, has evaluated and tested many different fuel cell systems, and is a part of the Advanced Power and Energy Program at UCI which investigates micro-turbine generators, gas turbines, photovoltaics and other renewable and advanced energy technologies. Thus the stage was set before the current contract for the NFCRC to provide California consumers, the market, students, faculty and staff the opportunity to understand and make informed decisions for the adoption of environmentally sensitive and energy efficient power generating technologies, such as fuel cells. The technology transfer infrastructure and technology transfer accomplished within this program directly exchanges the required information to accomplish the transfer of technology from the laboratory and development centers to the marketplace.

Technology transfer for fuel cells and fuel cell hybrid systems has been accomplished in the current program in three separate areas: (1) Multi-Functional Room, (2) EFAAM, and (3) NFCRC web site. The first technology transfer element (Multifunctional Room) included the design, purchase and installation of display and projection equipment, switching equipment, an integrated control system, technology transfer accommodations, and miscellaneous integration and control components. This task was accomplished in collaboration with the Intellisys Group. The second area of technology transfer accomplishments involved designing and installing an interactive educational facility for instruction and insight into both global climate change and urban air pollution issues. The third area of technology transfer accomplishments included a major design and implementation effort focused on the NFCRC web site.

The technology transfer features, whose development and implementation was supported in the current effort, were found to be most valuable for effective communication and information dissemination. The new features of the multi-functional room have been used often to inform, educate, and communicate both within the fuel cell community and between the fuel cell community and other groups spanning regulatory bodies, government agencies, other industries (related and non-related), research institutions, and the general public. The need and desire of these groups for objective, up-to-date, and useful information on fuel cells and hybrid systems was found to be large indeed, with an average of over 5 visits/week accommodated at the NFCRC primarily for technology transfer purposes. A key finding is that much larger efforts in this area are required to effectively engage the market to allow widespread adoption of fuel cells in California (and world-wide).

5.0 Conclusions and Recommendations

5.1 Conclusions

Since the current effort comprises only the first year of a three-year effort, key findings are limited, but valuable nonetheless. A major finding is that rigorous steady state analyses tools are not currently available for solid oxide fuel cells and hybrid systems. Preliminary results from the rigorous models developed in this effort are encouraging with regard to their ability to approximate conditions and results available in the literature without any adjustable parameters. The dependence of hybrid system components (SOFC, reformer, gas turbine) upon parametric variations is consistent with fundamental thermodynamics, efficiency expectations, and major loss mechanisms. The NFCRC has found the completed technology transfer features, whose development and implementation was supported in the current effort, to be most valuable to effective communication and information dissemination. The new features of the multi-functional room have been used often to inform, educate, and communicate both within the fuel cell community and between the fuel cell community and other groups spanning regulatory bodies, government agencies, other industries (related and non-related), research institutions, and the general public. The need and desire of these groups for objective, up-to-date, and useful information on fuel cells and hybrid systems was found to be large indeed, with an average of over five visits a week accommodated at the NFCRC primarily for technology transfer purposes. A key finding is that much larger efforts in this area are required to effectively engage the market to allow widespread adoption of fuel cells in California (and world-wide).

The current effort concludes that thermodynamic analysis tools for rigorous treatment, evaluation and design of fuel cells and hybrid systems are: (1) sorely needed and desired by the fuel cell research and development community, (2) not currently available, and (3) not currently packaged appropriately to allow the full flexibility that would be desired. Continued funding support of the out-years of this software development project is recommended to meet these needs. In addition, since fuel cell and hybrid technology is just now emerging from research, development and demonstration projects to commercial application, there is a need for continued technology transfer efforts. We recommend that the current technology transfer efforts receive continued support from the California Energy Commission, and encourage other entities (e.g., industry, agencies, laboratories) concerned about the adoption of these technologies in the marketplace to expand their efforts in similar technology transfer endeavors.

Conclusions drawn from this project were:

- Preliminary results from the rigorous models developed in this effort are encouraging with regard to their ability to approximate conditions and results available in the literature without any adjustable parameters.
- The dependence of hybrid system components (SOFC, reformer, gas turbine) upon parametric variations is consistent with fundamental thermodynamics, efficiency expectations, and major loss mechanisms.
- The NFCRC has found the completed technology transfer features to be most valuable to effective communication and information dissemination, both within the fuel cell community and between the fuel cell community and other groups.

5.2 Benefits to California

The project addresses the PIER program objective of reducing environmental and public health risks of California's electricity sector by helping develop environmentally preferred advanced generation technologies. Fuel cells and fuel cell hybrid technologies offer a remarkable opportunity to reduce environmental impact, increase energy efficiency, and lower electricity costs in the future. These technologies, however, are significantly different from currently available energy technologies, and face many hurdles to their widespread adoption that can only be overcome by concerted efforts to transfer this technology from research, development and demonstration to application in California.

5.3 Recommendations

We make the following recommendations:

- Funding the continued development of steady state analyses tools for fuel cells and fuel cell hybrid systems. Two additional years of funding support are required to finalize the analyses tools development, create a graphical user interface, and promulgate the use of these tools throughout the fuel cell community.
- Continued funding support of the out-years of the software development project to develop thermodynamic analysis tools for rigorous treatment, evaluation and design of fuel cells and hybrid systems.
- Current technology transfer efforts receive continued support from the California Energy Commission, and encourage other entities (e.g., industry, agencies, laboratories) concerned about the adoption of these technologies in the marketplace to expand their efforts in similar technology transfer endeavors.

6.0 Glossary

A/V	Audio/Visual
AC	Alternating current
APEP	Advanced Power and Energy Program
atm	Atmosphere
Btu	British thermal unit
Cermet	Ceramic metal
CH_4	Hydrocarbon
cm	Centimeter
CO	Carbon monoxide
CO_2	Carbon dioxide
Commission	California Energy Commission
$CoZrO_2$	Cobalt zirconium oxide
DC	Direct current
DOE	U. S. Department of Energy
DTTF	Distributed Technologies Testing Facility
DVD	Digital video disc
EFAAM	Educational Facility for Ambient Air Monitoring

GASTURB	Gas turbine
H_2	Hydrogen
H_2O	Water
HHV	Higher heating value
HTS	High temperature shift
Hz	Hertz
ISO	International Organization for Standardization
kg/s	Kilograms
kWh	Kilowatt hour
L2	Living Laboratory
$LaMnO_3$	Lanthanum permanganate
LHV	Lower heating value
LTS	Low temperature shift
mA	Milliampere
MCFC	Molten Carbonate Fuel Cell
MF	Multi-Functional room
MW	Megawatt
NFCRC	National Fuel Cell Research Center

$NiZrO_2$	Nickel zirconium oxide
NO_x	Nitrogen oxide
NTSC	National Television System Committee
O_2	Oxygen
O_3	Ozone
PAFC	Phosphoric Acid Fuel Cell
PARCON	Pacific Rim Consortium on Energy Combustion and the Environment
PEMFC	Proton Exchange Membrane Fuel Cell
PIER	Public Interest Energy Research
ppmV	Parts per million by volume
psia	Pounds per square inch absolute
PVEA	Petroleum Violation Escrow Account
RD&D	Research, development and demonstration
S/C	Steam-to-carbon ration
SCAQMD	South Coast Air Quality Management District
SOFC	Solid oxide fuel cell
Sr	Strontium
SWPC	Siemens Westinghouse Power Corporation

UCI	University of California at Irvine
UCICL	University of California Irvine Combustion Laboratory
V	Volt
Y_2O_3	Yttria (Yttrium oxide)
ZrO_2	Zirconia (Zirconium oxide)

7.0 References

1. Achenbach, E., "Three-dimensional and time-dependent simulation of a planar solid oxide fuel cell stack," Journal of Power Sources, Vol.49, pp. 333-348 (1994).
2. Adler et al., Electrode Kinetics of Porous Mixed-Conducting Oxygen Electrodes, *J. of The Electrochemical Society*, Vol. 143, pp. 3554, 1996.
3. Alatiqi, I. M., A. M. Meziou, and G. A. Gasmelseed, "Modelling Simulation and Sensitivity Analysis of Steam-Methane Reformers," Int. J. Hydrogen Energy, 14, 241-256 (1989).
4. Alatiqi, I. M., and A. M. Meziou, "Dynamic Simulation and Adaptive Control of an Industrial Steam Reformer," Computers chem. Engng, 15, 147-155 (1991).
5. Andrew, M.R., "Chapter 4, Kinetic Effects--Part 2," in An Introduction to Fuel Cells, ed. K.R. Williams, Elsevier Publishing Company, New York, (1966).
6. Appleby, A.J. and Foulkes, F.R., Fuel Cell Handbook, Krieger Publishing Company, Florida, p 602, 1993.
7. Belzner, A., et al., Oxygen Chemical Diffusion in Strontium Doped Lanthanum Manganites, *Solid State Ionics V*, Vol. 57, No. 3-4, pp. 327-337, October 1992.
8. Bessette, N. F. and George, R.A., Performance and Reliability of Westinghouse's Air Electrode Supported Solid Oxide Fuel Cell at Atmospheric and Elevated Pressures, 1996.
9. Bessette, N..F., Modeling and Simulation for Solid Oxide Fuel Cell Power Systems, Ph.D. Thesis, Georgia Institute of Technology, July 1994.
10. Bevc, F.P. and Parker, W.G., SureCell™ Integrated Solid Oxide Fuel Cell Power Plants for Distributed Power Applications, PowerGen 1995 Americas, December 5-7, 1995.
11. Bird, R.B., et al., Transport Phenomena, John Wiley & Sons, New York, pp 674-675, 1960.
12. Brown, M., et al., Structure/Performance Relations for Ni/Yttria-Stabilized Zirconia Anodes for Solid Oxide Fuel Cells, *J. of The Electrochemical Society*, Vol.147, No. 2, pp. 475-485, 2000.
13. Carberry, J.J., Chemical and Catalytic Reaction Engineering, McGraw-Hill, New York, p 491, 1976.
14. Cohen et al., Fuel Cell Power Plant with Increased Reactant Pressures, U.S. Patent 4,743,517 (1988).
15. Deng, H. et al., Diffusion-Reaction in Mixed Ionic Electronic Conductor Solid Oxide Membrane with Porous Electrodes, *Solid State Ionics IV*, Symposium Proceedings, Vol. 369, pp. 415-420, November-December 1994.
16. Divisek, J. et al., The kinetics of Electrochemical Reactions on High Temperature Fuel Cell Electrodes, *J. of Power Sources*, Vol. 49, pp. 257-270, 1994.
17. Dunbar, W.R., and Gaggioli, R.A., Modeling of Solid Electrolyte Fuel Cells, A Future for Energy, S. Stecco, ed., Pergamon Press, Oxford, 1983.

18. Electric Research Institute's Technical Assessment Guide, Report No. P-2410-SR, May 1982.

19. El-Masri, M.A. and Pourkey, F., Prediction of Cooling Flow Requirements for Advanced Utility Gas Turbines Part 1: Analysis and Scaling of the Effectiveness Curve, presented at the Winter Annual Meeting of the ASME, December 1986.

20. Elshof, M. H, et al., Oxygen Exchange and Diffusion Coefficients of Strontium-Doped Lanthanum Ferrites by Electrical Conductivity Relaxation, *J. of The Electrochemical Society*, Vol. 144, No. 3, pp. 1060-1067, 1997.

21. Enick et al., High Pressure Humidification Columns: Design Equations, Algorithm, and Computer Code, Technical Report, DOE/PETC/TR-94-05, 1994.

22. Facts and Figures, International Energy Agency SOFC Task Report, Swiss Federal Office of Energy, Berne, 1992

23. Fee, D.C., Zwick, S.A., and Ackerman, J.P., Proceedings of the Conference on High Temperature Solid Oxide Electrolytes, Brookhaven National Laboratory, August 16-17, 1983, BNL 51728, compiled by F.J. Slazano, October, 1983.

24. Ferguson, J.R., Heat and Mass Transfer Aspects of SOFC Assemblies and Systems, IEA Natural Gas Fueled Solid Oxide Fuel Cells and Systems, July 2-6, 1989.

25. Fogler, H. S., Elements of Chemical Reaction Engineering, Prentice Hall, New Jersey, 1986.

26. Foust, A.S. et al., Principles of Unit Operations, Second Edition, John Wiley & Sons, New York, pp 428-449, 1980.

27. Gas Research Institute Report, Evaluation of Advanced Gas Turbine Cycles, GRI-93/0250, August 1993.

28. Gillespie et al., Vapor-liquid Equilibrium Data on Water-substitute Gas Components, Gas Processors Association, Research Report RR-41, April 1980.

29. Gur, T. M., et al., A New Class of Oxygen Selective Chemically Driven Nonporous Ceramic Membranes, Part I, A-site Doped Perovskites, *J. of Membrane Science*, Vol. 75, pp. 152-162, 1992.

30. Haynes, C. L., Simulation of Tubular Solid Oxide Fuel Cell Behavior for Integration Into Gas Turbine Cycles, Ph.D. Thesis, Georgia Institute of Technology, July 1999.

31. He, W., "Dynamic Response of a Reformer for Molten Carbonate Fuel Cell Power-Generation Systems," Fuel Processing Technology, 53, 99-113 (1997).

32. Hirano, A. et al., Evaluation of a New Solid Oxide Fuel Cell System by Non-isothermal Modeling, *J. of The Electrochemical Society*, Vol. 139, No. 10, October 1992.

33. Hirschenhofer, J.H., et al., Fuel Cell Handbook (Revision 3), U.S. Department of Energy (DE94004072), January 1994

34. Hottel, H.C., and Sarofim, A.F., Radiative Transfer, McGraw-Hill, New York, 1967.

35. Ihara, M. et al., Effect of the Steam-Methane Ratio on Reactions Occurring on Ni/Yttria-Stabilized Zirconia Cermet Anodes Used in Solid-Oxide Fuel Cells, *J. of The Electrochemical Society*, Vol.146, No. 7, pp. 2481-2487, 1999.

36. International Energy Agency Report, Electricity Production and CO_2 Capture via Partial Oxidation of Natural Gas, August 1999.

37. JANAF Thermochemical Tables, *J. of Physical Chemistry Ref. Data*, Vol. 14, Suppl.1, 1985.

38. Kanamura, K. et al. Temperature Distribution in Tubular Solid Oxide Fuel Cell, International Symposium on Solid Oxide Fuel Cells, Published by the Electrochemical Society, 1989.

39. Kern, D.Q., Process Heat Transfer, McGraw Hill, New York, pp. 563-621, 1950.

40. Kim, J., et al., Polarization Effects in Intermediate Temperature, Anode-Supported Solid Oxide Fuel Cells, *J. of The Electrochemical Society*, Vol. 146, No. 1, pp. 69-78, 1999.

41. Kortbeek, P. J., de Ruijter, J. A. F., van der Laag, P. C., Barten, H., "A Dynamic Simulator for a 250 kW class ER-MCFC system," Journal of Power Sources, Vol. 71, pp. 278-780 (1998).

42. Lane, J. A., et al., Development and Evaluation of Oxide Cathodes for Ceramic Fuel Cell Operation at Intermediate Temperatures, *British Ceramic Proceedings*, 1995.

43. Levenspiel, O., Chemical Reaction Engineering, 2nd Edition, John Wiley & Sons, New York, 1972.

44. Levy, et al., Hydrogen Fuel Reforming in a Fog Cooled Fuel Cell Power Plant Assembly, U.S. Patent 4,865,926 (1989).

45. Lukas, M.D., K.Y. Lee, and H. Ghezel-Ayagh, "Development of a Stack Simulation Model for Control Study on Direct Reforming Molten Carbonate Fuel Cell Power Plant," Submitted to IEEE Power Engineering Society, 1999 Winter Meeting, New York, NY.

46. Marks' Standard Handbook for Mechanical Engineers, Editors: Avallone, E.A. and Baumeister, T., 10th Edition, McGraw Hill, New York, 1996.

47. Matsuzaki,Y. and Yasuda, I., Electrochemical Oxidation of H_2 and CO in a H_2- H_2O-CO-CO_2 System at the Interface of a Ni-YSZ Cermet Electrode and YSZ Electrolyte, *J. of The Electrochemical Society*, Vol.147, No. 5, pp. 1630-1635, 2000.

48. McCabe, W.L. and Smith, J.C., Unit Operations of Chemical Engineering, Third Edition, Chemical Engineering Series, McGraw Hill, New York, 1976, pp 744-770.

49. Ong, B.G. et al., The Anodic Oxidation of H2 and H2S on Yttriaria Stabilized Zirconia (YSZ) with Porous Au, Ni and Pt Metal Electrodes, *2nd Symposium on Electrode Materials*, Vol. 87-12, 1987.

50. Park, S. et al., Direct Oxidation of Hydrocarbons in a Solid Oxide Fuel Cell – I. Methane Oxidation, *J. of The Electrochemical Society*, Vol.146, No. 10, pp. 3603-3605, 1999.

51. Patankar, S.V., Numerical Heat Transfer and Fluid Flow, Hemisphere Publishing Corp., New York (1980).

52. Peng, D. and Robinson, D.B., A New Two-constant Equation of State, *Industrial Engineering Chemistry Fundamentals*, Vol. 116, No. 1, pp. 59-64, 1976

53. Pizzini,S., Fast Ion Transport I Solids, Solids State Batteries and Devices, W. van Gool, Editor, p. 461, North-Holland Publishing Company, Amsterdam, 1973.

54. Primdahl, S. and Mogensen, M., Gas Diffusion in Characterization of Solid Oxide Fuel Cell Anodes, *J. of The Electrochemical Society*, Vol.146, No. 8, pp 2827-2833, 1999.

55. Rao, A. D., Process for Producing Power, U.S. Patent No. 4,289,763, May 16, 1989.

56. Reid, R.C., et al., The Properties of Gases and Liquids, McGraw Hill, New York, Appendix A, 1984.

57. Sasaki, K., et al., Microstructure-Property Relations of Solid Oxide Fuel Cell Cathodes and Current Collectors, *J. of The Electrochemical Society*, Vol. 143, No. 2, pp. 530-543, 1996.

58. Schnackel, H.C., Formulations for the Thermodynamic Properties of Steam and Water, *Transactions of the ASME*, pp. 959-966, May 1958.

59. Shingai et al., Fuel Cell/Gas Turbine Combined Power Generation System and Method for Operating the Same, U.S. Patent 5,482,791 (1996).

60. Spencer, R.C. et al., A Method for Predicting the Performance of Steam Turbine-Generators, General Electric Technical Bulletin GER –2007C, July 1974.

61. Svensson, A. M., et al., Mathematical Modeling of Oxygen Exchange and Transport in Air-Perovskite-YZS Interface Regions, *J. of The Electrochemical Society*, Vol. 144, No. 8, pp 2719-2732, 1997.

62. Takahashi, T. et al., *Third International Symposium on Fuel Cells*, p. 113, Presses Academiques Europeenes, Bruxelles, 1969.

63. Turgut, M., et al., A New Class of Oxygen Selective Chemically Driven Nonporous Ceramic Membranes, Part I, A-site Doped Perovskites, *J. of Membrane Science*, Vol. 76, pp 151-162, 1992.

64. U.S. DOE Report, Annual Energy Outlook 1998, with Projection to 2020, DOE/EIA-0383(98), December 1997.

65. U.S. DOE Report, International Energy Outlook 1996, DOE/IEO96, 1996.

66. Vogler, T.C. and Weissman, W., Thermodynamic Availability Analysis for Maximizing a System's Efficiency, *Chemical Engineering Progress*, Vol. 84, No. 3, pp35-42, 1988.

67. Wepfer, W.J., and Woolsey, M.H., High Temperature Fuel Cells for Power Generation, *Energy Conversion Management*, Vol. 25, 1985.

68. Wohr, M, K. Bolwin, W. Schnurnberger, M. Fischer, W. Neubrand, and G. Eigenberger, "Dynamic Modeling and Simulation of a Polymer Membrane Fuel Cell Including Mass Transport Limitation," Int. J. Hydrogen Energy, 23, 3, pp. 213-218 (1998).

69. Young, H. D., Fundamentals of Optics and Modern Physics, McGraw-Hill, New York, 1968.

Appendix I

Energy Tutorial HTML Document

http://www.nfcrc.uci.edu/EFAAM

Appendix II

Presentation Materials for EFAAM Displays